



# Incorporating Planetary Space Environments into the Basilisk Astrodynamics Framework

Hanspeter Schaub, *Professor, Glenn L. Murphy Chair of Engineering*

Patrick Kenneally, *Software Systems Architect, Mission Modeling and Verification, JPL*

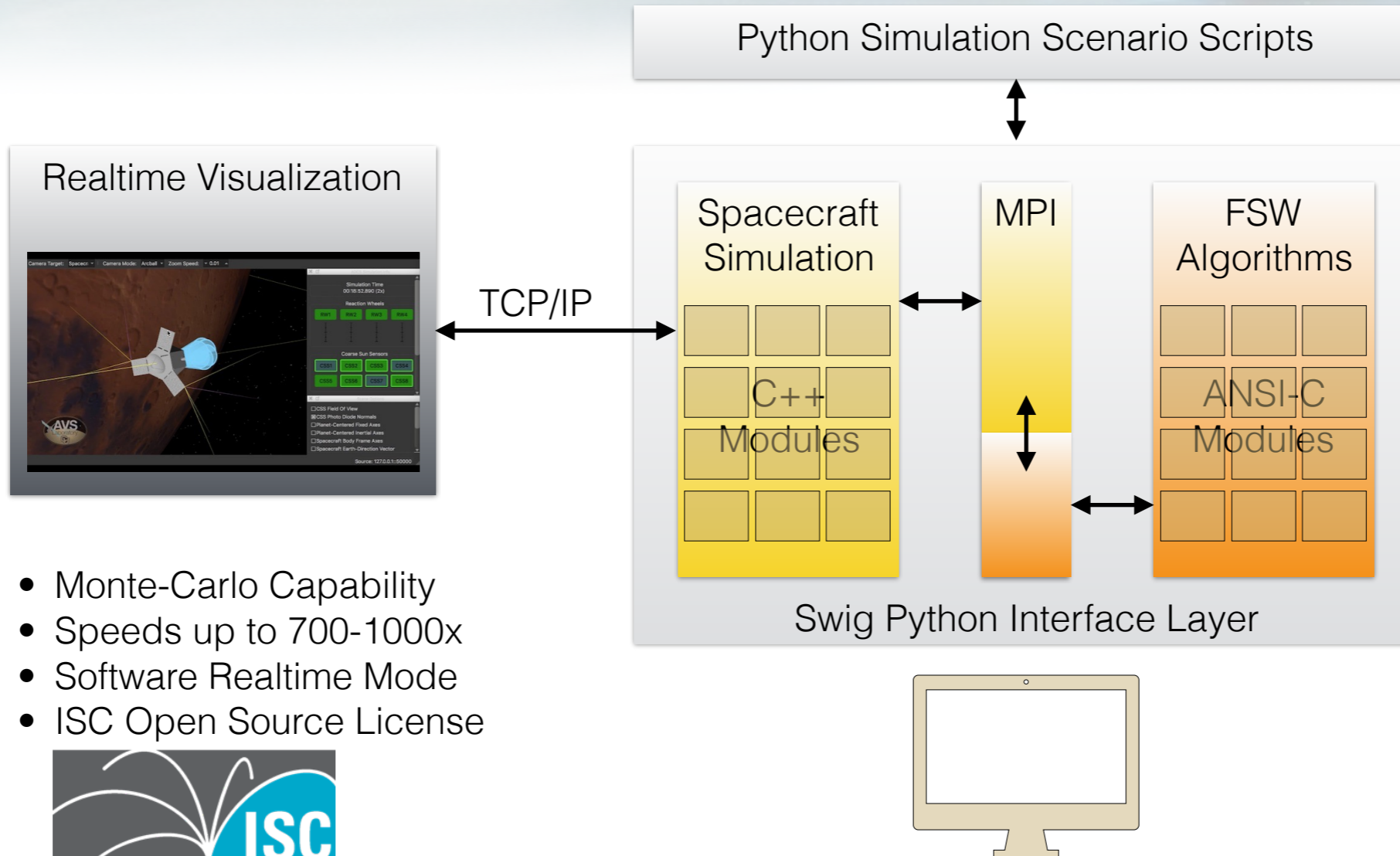
Andrew Harris, *Graduate Research Assistant*

Advances and Applications of Computational Astrodynamics , APCOM 2019, Taipei, Taiwan



Ann and H. J. Smead Aerospace  
Engineering Sciences Department  
University of Colorado, **Boulder**

# Basilisk Software Architecture



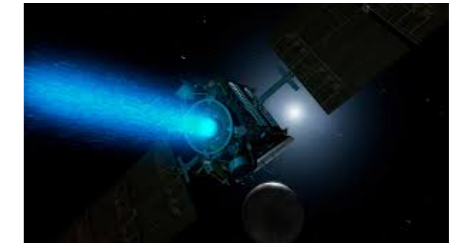
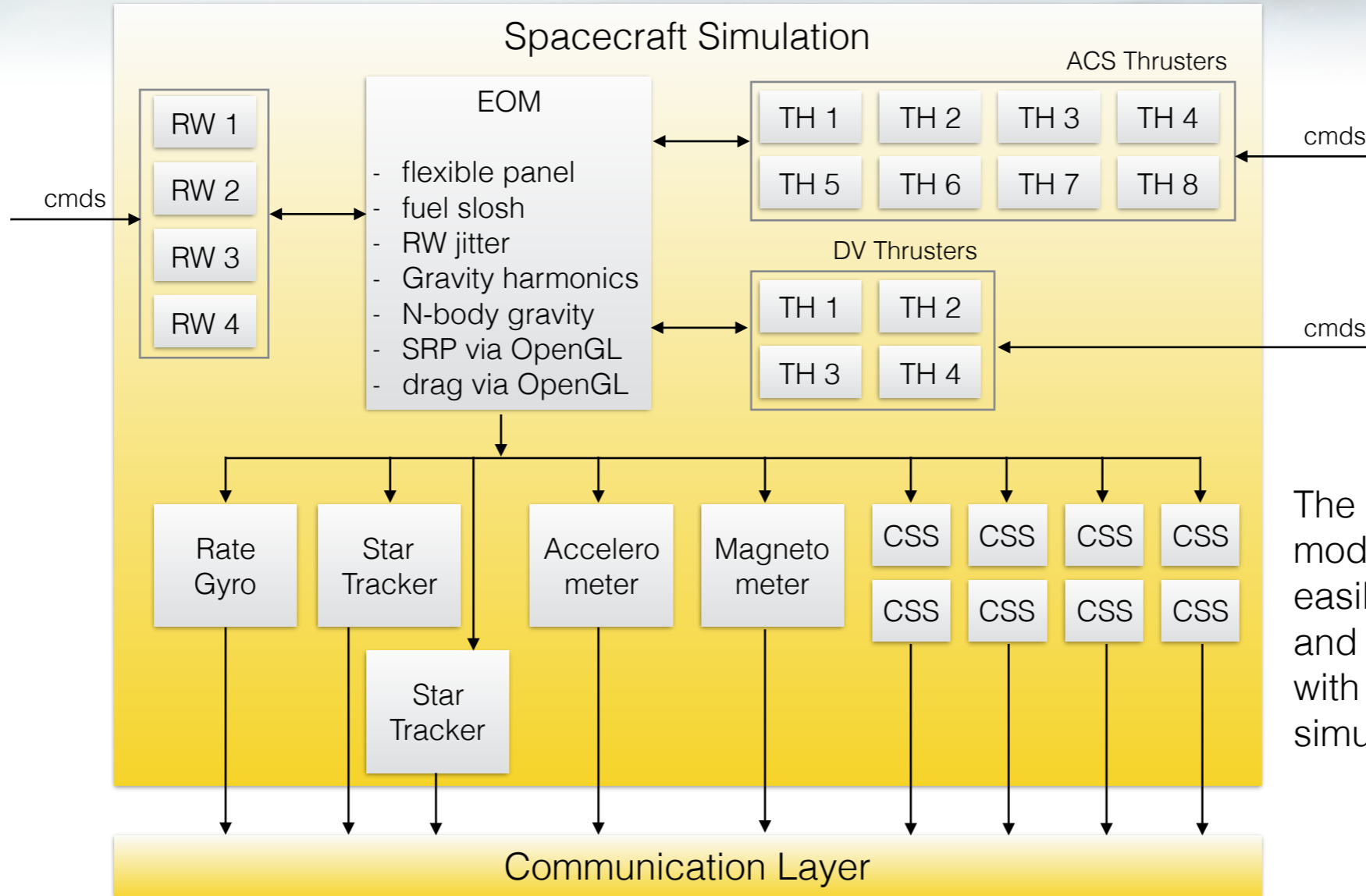
- Monte-Carlo Capability
- Speeds up to 700-1000x
- Software Realtime Mode
- ISC Open Source License



P. Kenneally, H. Schaub and S. Piggott, "Basilisk: A Flexible, Scalable and Modular Astrodynamics Simulation Framework," 7th International Conference on Astrodynamics Tools and Techniques (ICATT), DLR Oberpfaffenhofen, Germany, November 6–9, 2018.

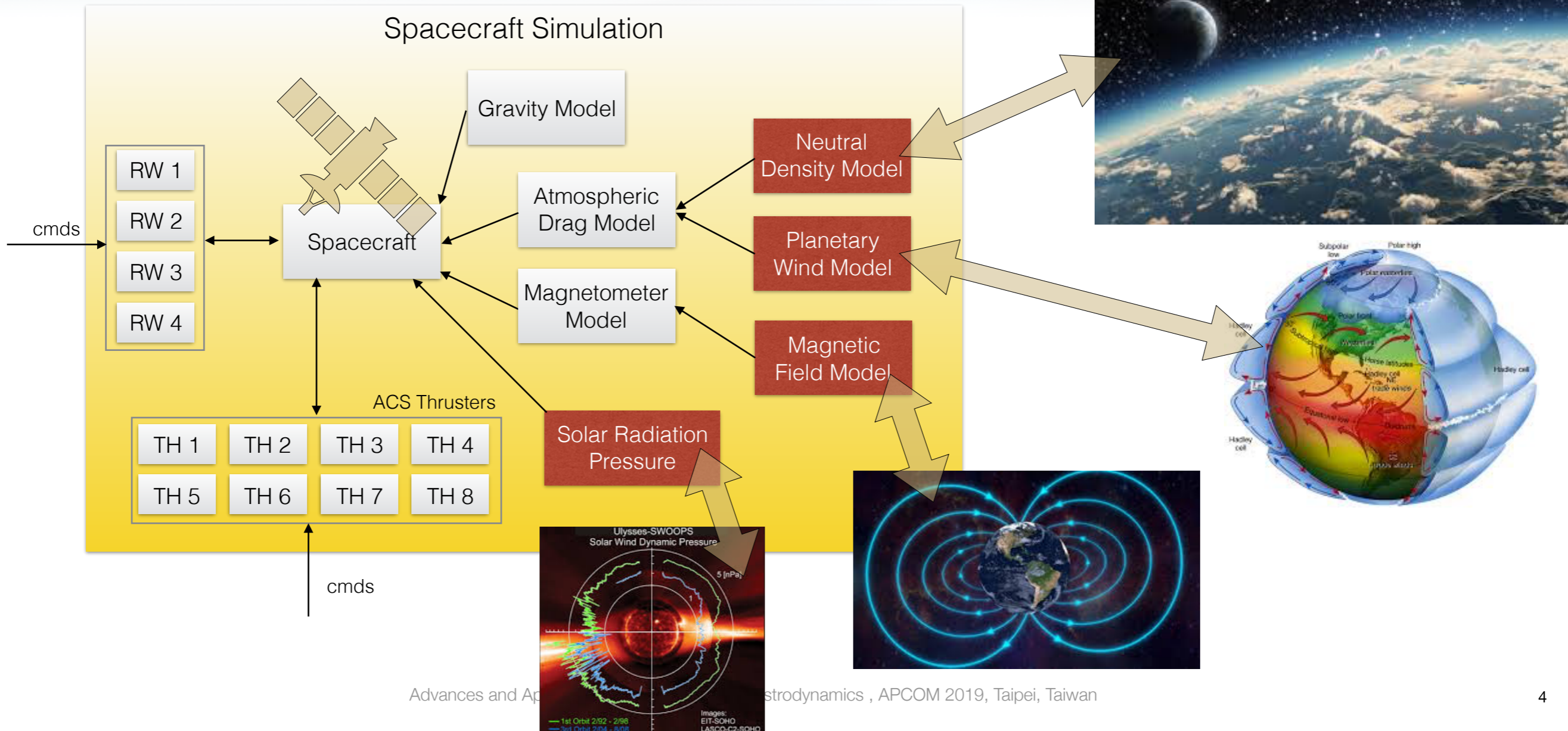
Advances and Applications of Computational Astrodynamics , APCOM 2019, Taipei, Taiwan

# Sample Spacecraft Simulation Setup



The C++ device modules can easily be added and connected with the the simulation.

# Spacecraft Environment Integration





## Magnetic field Models:

- centered dipole model
- WMM



## Neutral Density Models:

- exponential atmosphere
- MSIS

# MagneticFieldBaseClass: I/O Messages



# MagneticFieldBaseClass: Methods



```
class MagneticFieldBase: public SysModel {  
  
public:  
    void SelfInit();  
    void CrossInit();  
    void Reset(uint64_t CurrentSimNanos);  
    void addSpacecraftToModel(std::string  
                               tmpScMsgName);  
    void UpdateState(uint64_t CurrentSimNanos);  
  
    std::vector<std::string> scStateInMsgNames;  
    std::vector<std::string> envOutMsgNames;  
    std::string planetPosInMsgName;  
    double envMinReach;  
    double envMaxReach;  
    double planetRadius;
```

```
protected:  
    void writeMessages(uint64_t CurrentClock);  
    bool readMessages();  
    void updateLocalMagField(double currentTime);  
    void updateRelativePos(SpicePlanetStateSimMsg  
                           *planetState, SCPlusStatesSimMsg *scState);  
  
    virtual void evaluateMagneticFieldModel(  
        MagneticFieldSimMsg *msg,  
        double currentTime) = 0;  
    virtual void customSelfInit();  
    virtual void customCrossInit();  
    virtual void customReset(uint64_t  
                               CurrentClock);  
    virtual void customWriteMessages(uint64_t  
                                       CurrentClock);  
    virtual bool customReadMessages();
```

```
void MagneticFieldCenteredDipole::evaluateMagneticFieldModel(MagneticFieldSimMsg *msg, double currentTime)
{
    Eigen::Vector3d magField_P;           // [T] magnetic field in Planet fixed frame
    Eigen::Vector3d rHat_P;               // [] normalized position vector in E frame components
    Eigen::Vector3d dipoleCoefficients; // [] The first 3 IGRF coefficient that define the magnetic dipole

    //! - compute normalized E-frame position vector
    rHat_P = this->r_BP_P.normalized();

    //! - compute magnetic field vector in E-frame components (see p. 405 in doi:10.1007/978-1-4939-0802-8)
    dipoleCoefficients << this->g11, this->h11, this->g10;
    magField_P = pow(this->planetRadius/this->orbitRadius,3)*(3* rHat_P*rHat_P.dot(dipoleCoefficients)
        - dipoleCoefficients);

    //! - convert magnetic field vector in N-frame components and store in output message
    m33tMultV3(this->planetState.J20002Pfix, magField_P.data(), msg->magField_N);

    return;
}
```





## Epoch States:

- BSK default 2019-01-01, 00:00:00
- Set from Python directly within the module
- Read in through an optional epoch input message

```
class MagneticFieldWMM: public MagneticFieldBase {
public:
    MagneticFieldWMM();
    ~MagneticFieldWMM();

private:
    void evaluateMagneticFieldModel(MagneticFieldSimMsg *msg, double currentTime);

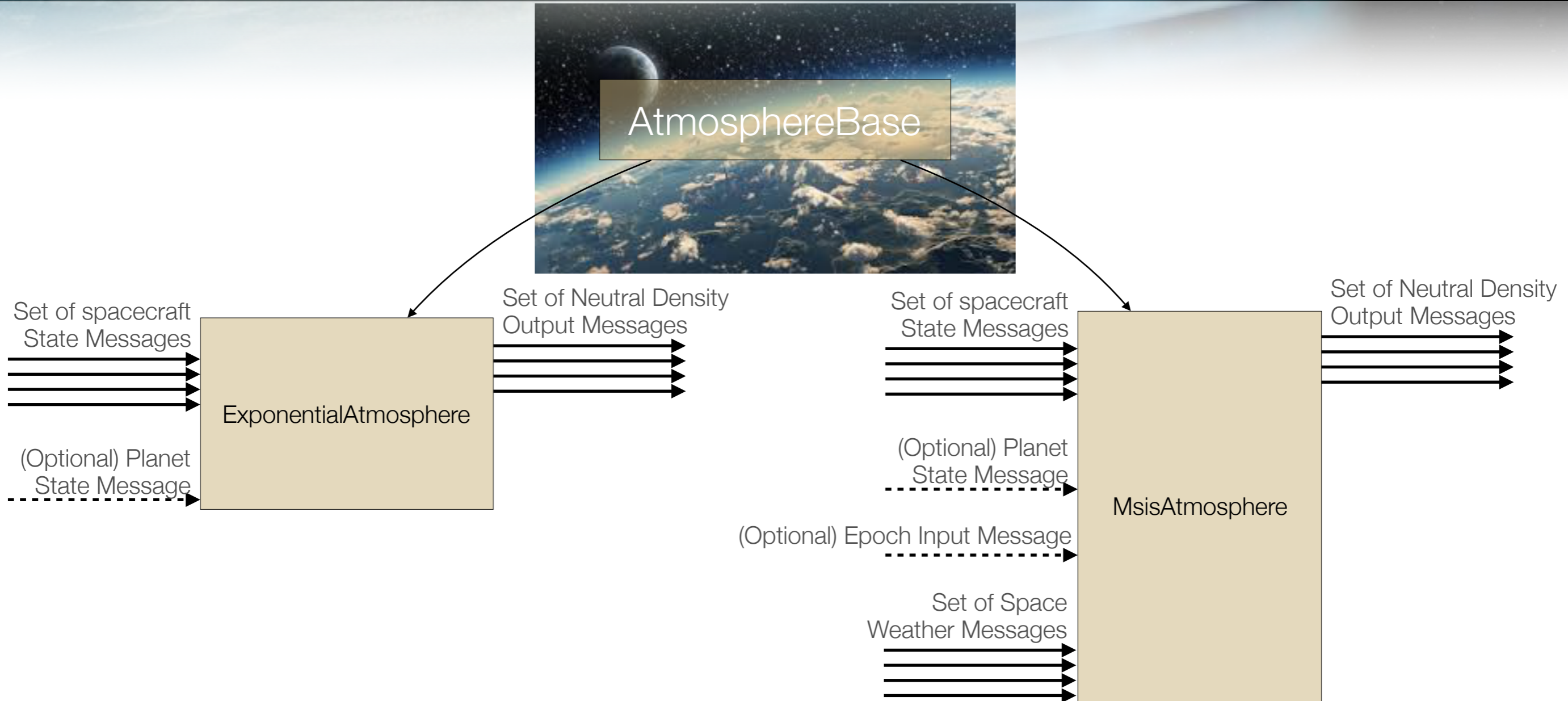
    void initializeWmm(const char *dataPath);
    void cleanupEarthMagFieldModel();
    void computeWmmField(double decimalYear, double phi, double lambda, double h, double B_M[3]);

    void customReset(uint64_t CurrentClock);
    void customCrossInit();
    void customSetEpochFromVariable();

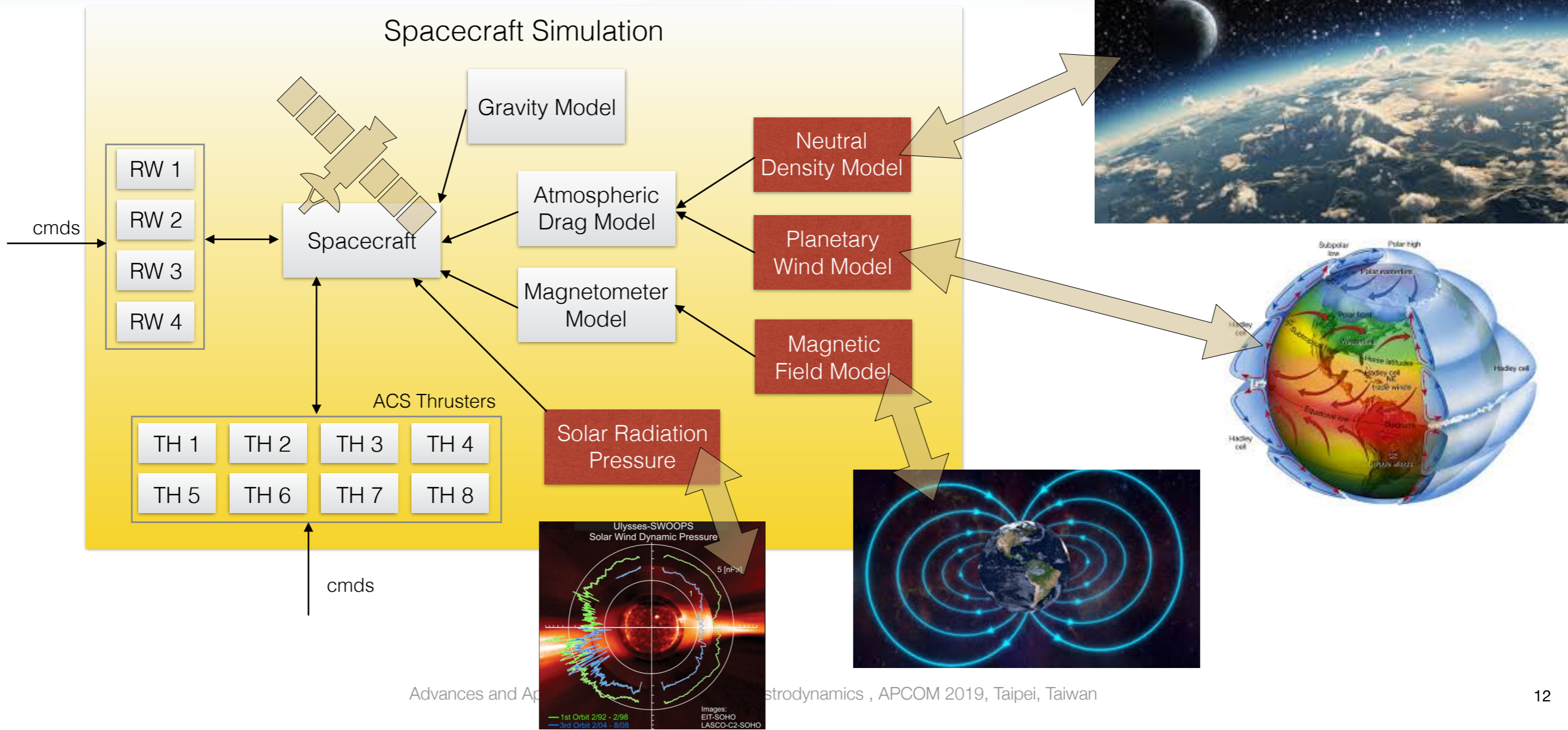
    void decimalYear2Gregorian(double fractionalYear, struct tm *gregorian);
    double gregorian2DecimalYear(double currentTime);

public:
    std::string epochInMsgName;           //!< -- Message name of the epoch message
    std::string dataPath;                 //!< -- String with the path to the WMM coefficient file
    double epochDateFractionalYear;      //!< -- Specified epoch date as a fractional year
```

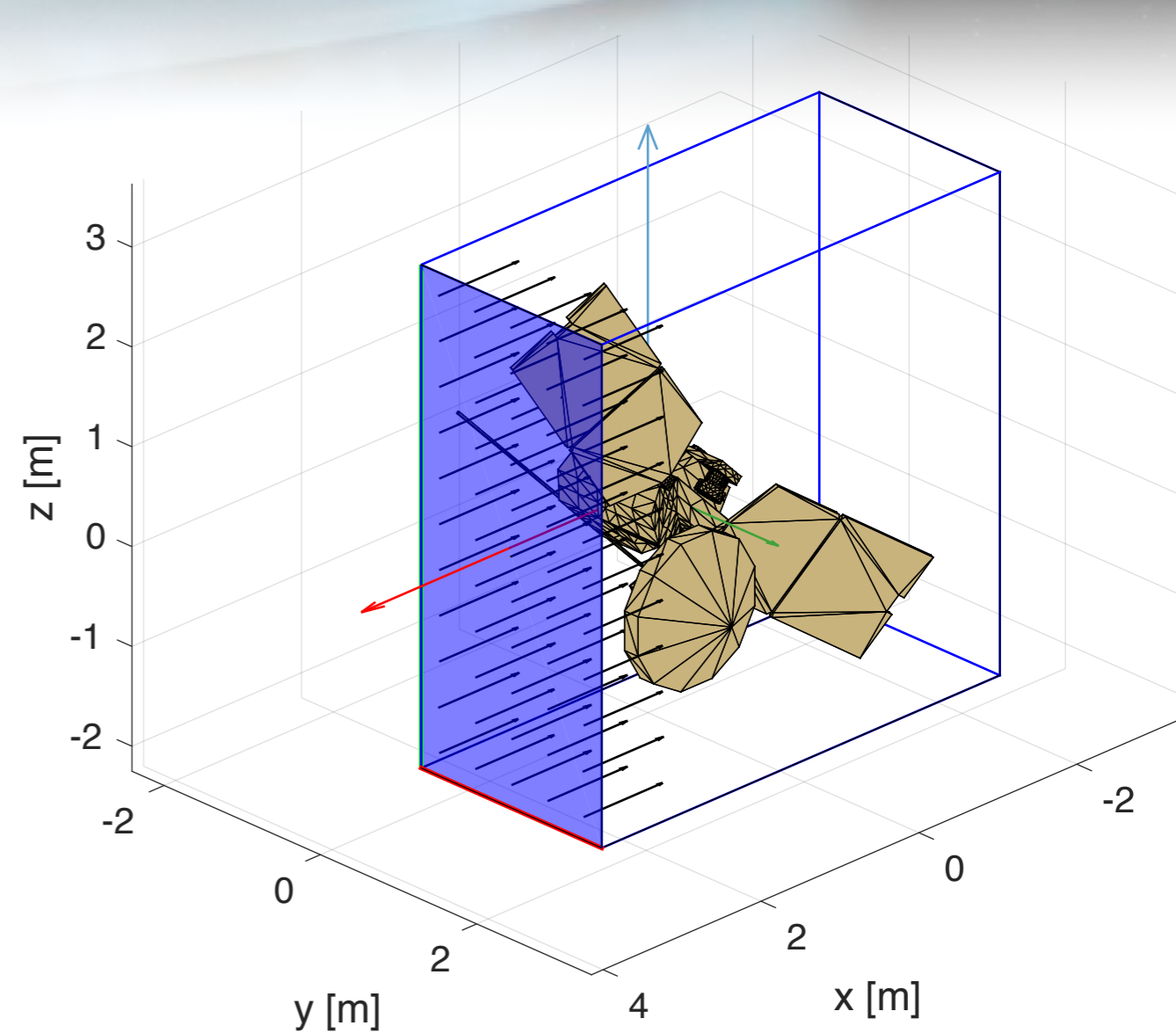
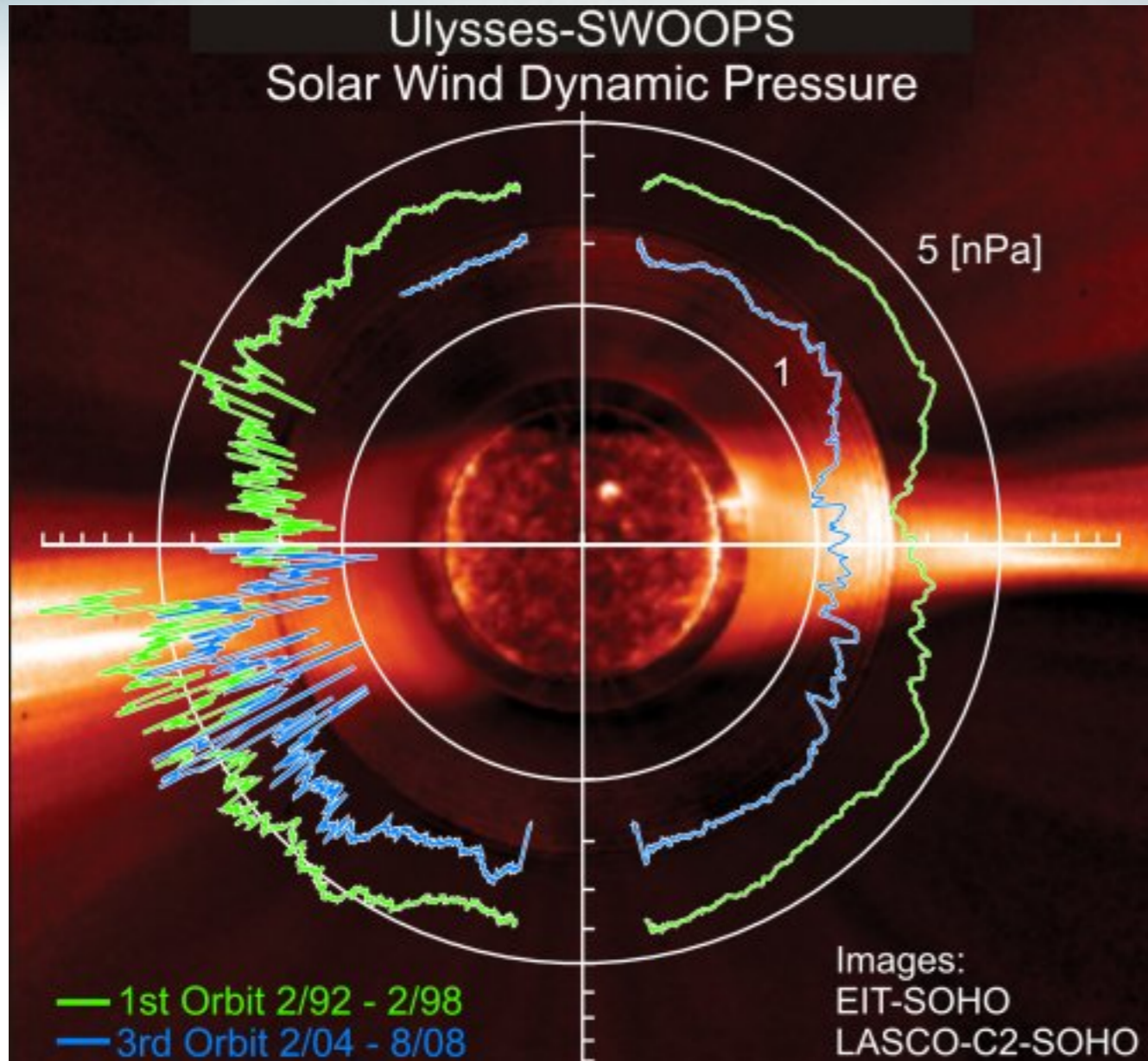
# Neutral Atmospheric Density Modeling



# Spacecraft Environment Integration



# Solar Radiation Pressure Modeling



# GPU Usage for Solar Radiation Pressure Modeling

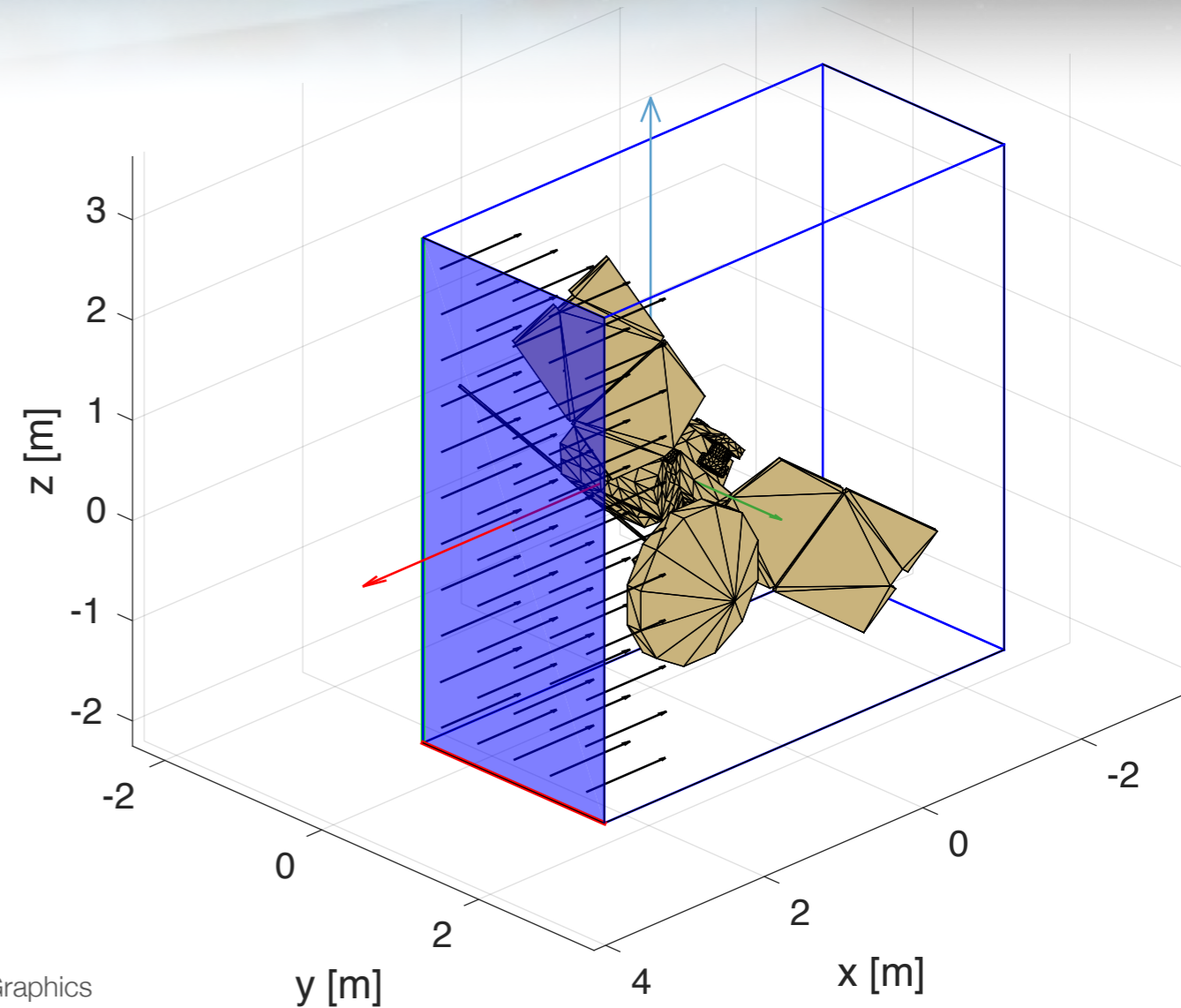


- Setup:

- Use full CAD Model
- Add SRP properties to surface texture

- Usage:

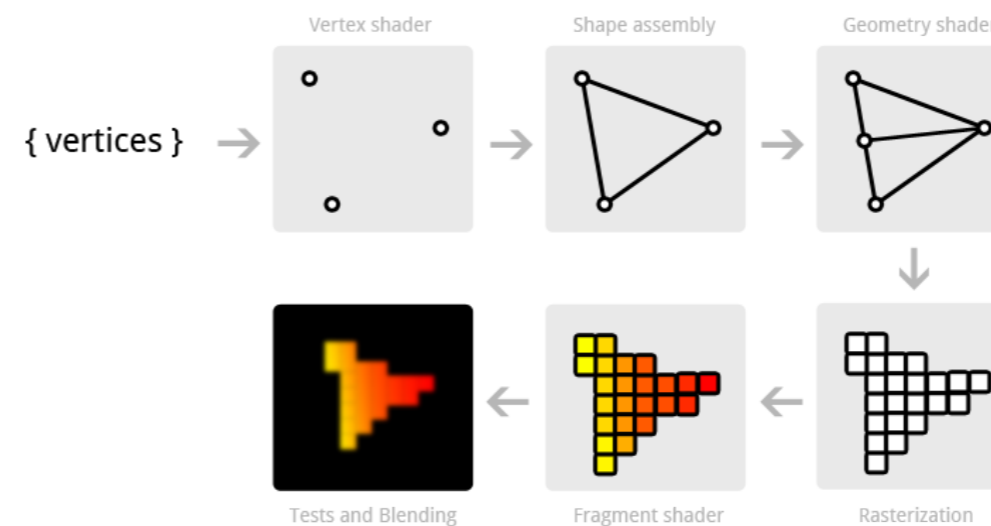
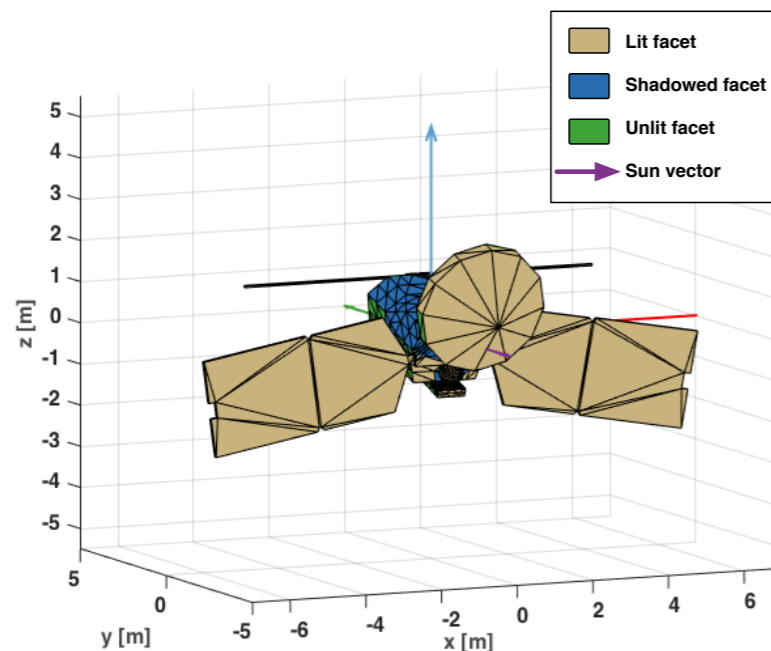
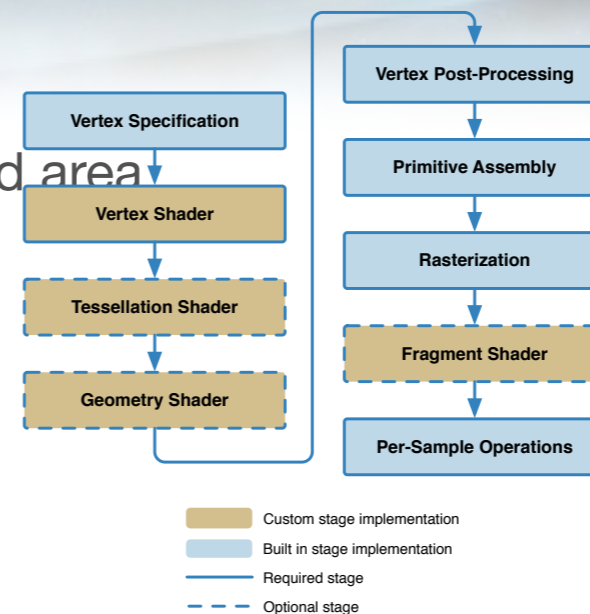
- Within Basilisk this model is loaded up once onto the GPU.
- Can handle time varying geometries through the use of articulated mesh structures
- Each time step the orientation relative to the solar flux is adjusted based on the current spacecraft orientation
- The forces acting on each CAD facet are added up to yield a net force and torque



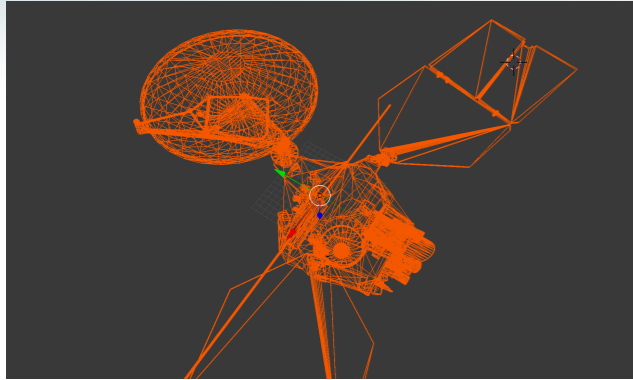
P. Kenneally and H. Schaub, "Modeling Of Solar Radiation Pressure and Self-Shadowing Using Graphics Processing Unit," AAS Guidance, Navigation and Control Conference, Breckenridge, Feb. 2-8, 2017.

# Faceted SRP Using OpenGL Render Pipeline

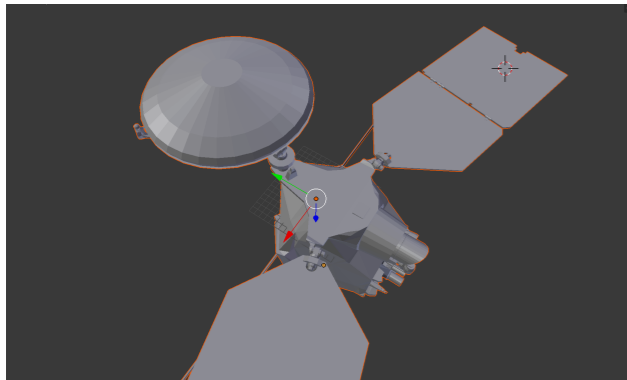
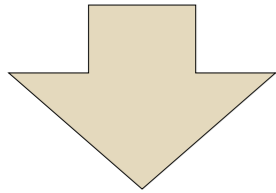
- Use built in OpenGL depth testing
- Use built in OpenGL rasterization to generate sun projected area
- OpenGL-CL shared data context



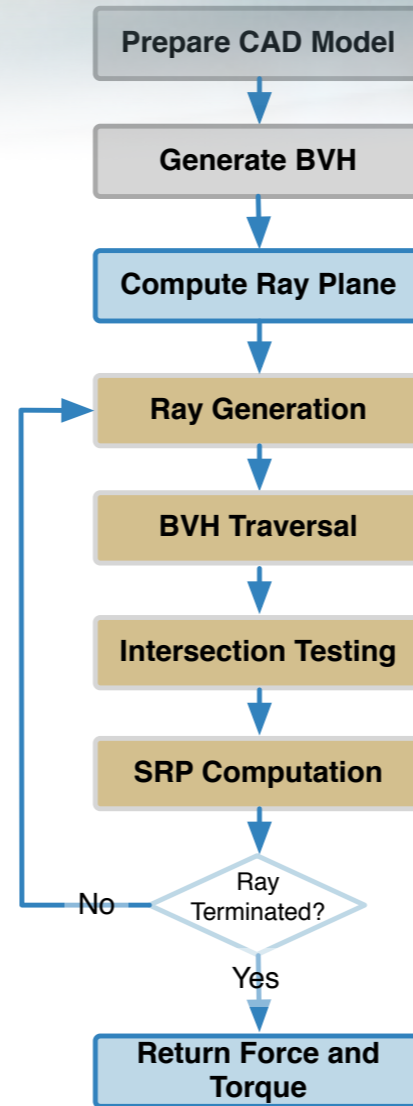
# GPU Based Solar and Atmospheric Pressure Drag



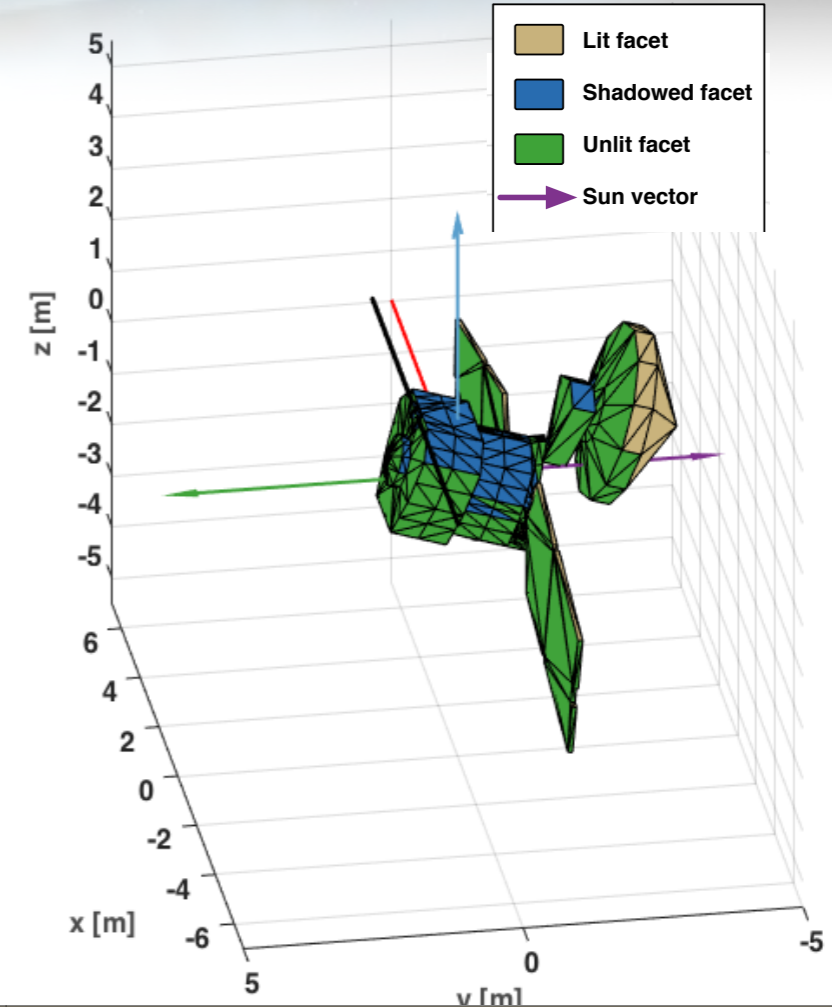
CAD model with material properties



Use GPU to evaluate forces and torques using custom vertex shaders



- GPU OpenCL execution
- CPU execution
- CPU initialization execution



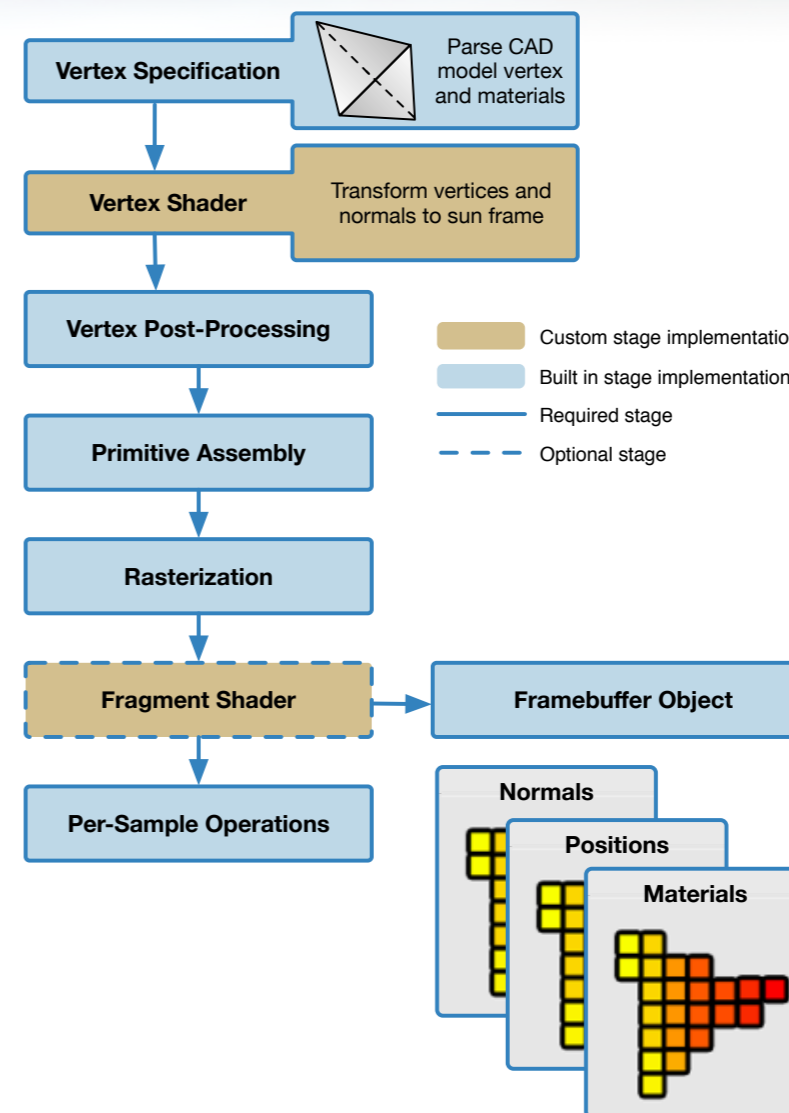
Drag forces can be rapidly computed on complex, time-varying geometries at speeds suitable for even hardware in-the-loop scenarios.

P. Kenneally and H. Schaub, "High Geometric Fidelity Modeling Of Solar Radiation Pressure Using Graphics Processing Unit," *AAS Spaceflight Mechanics Meeting*, Napa Valley, California, February 14–18, 2016. Paper No. 16-500.



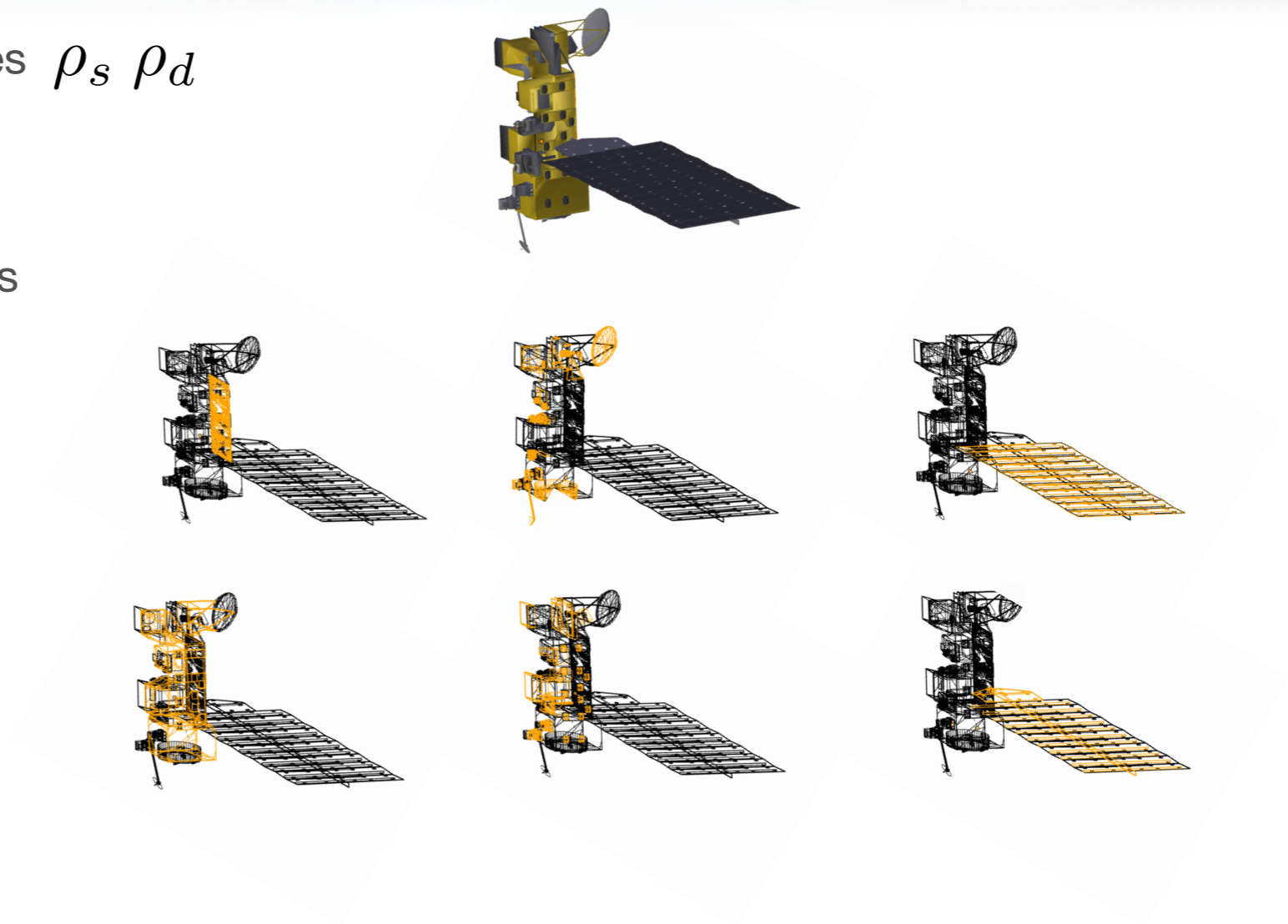
# Custom OpenGL Render Pipeline

- Framebuffer Object holds the rendered output
- Textures objects (typically used for 2D image data) are attached to the Framebuffer
- Vertex Shader performs a series of frame transformations from body-frame to projection-frame
- Each vertex's position vector, normal vector and material definition is passed through
- Fragment Shader outputs sun lit model regions



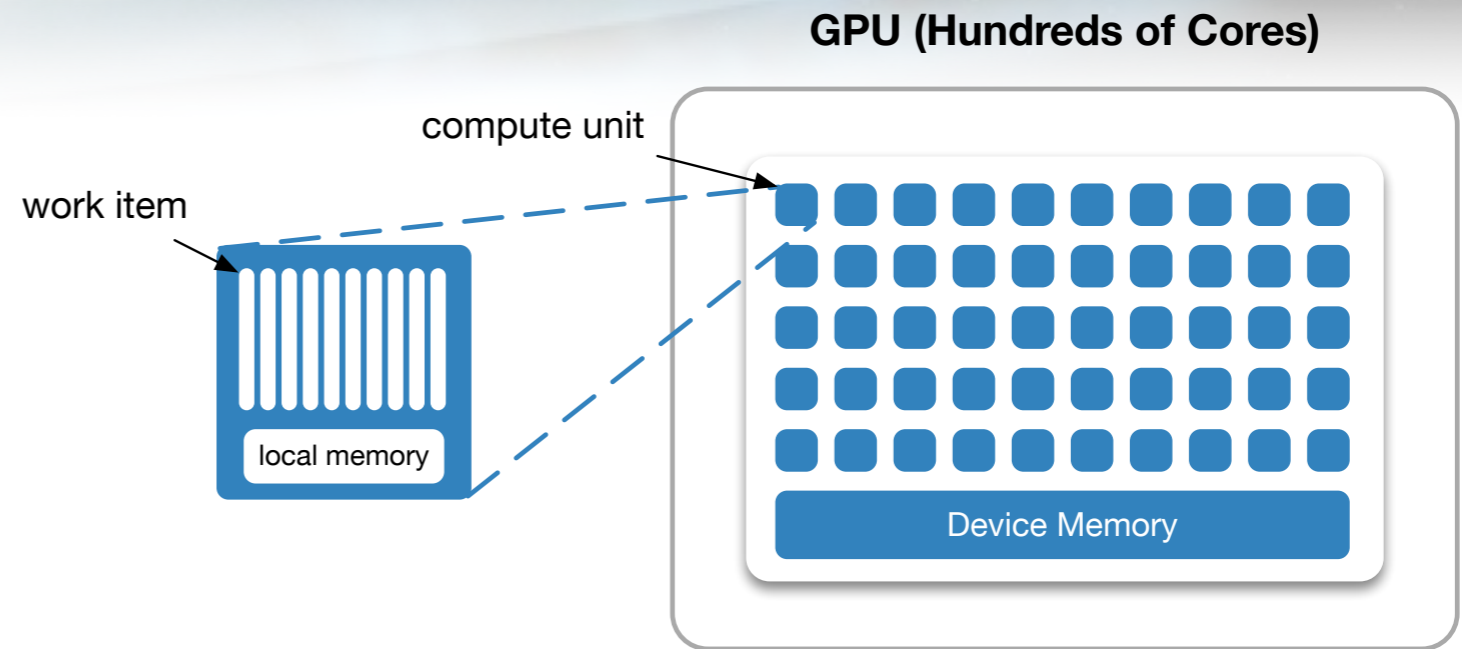
# Mesh and Material Definition

- .OBJ and .MTL files
- Each facet allocated material properties  $\rho_s$   $\rho_d$
- Sub-meshes defined recursively
- A mesh may have multiple sub-meshes



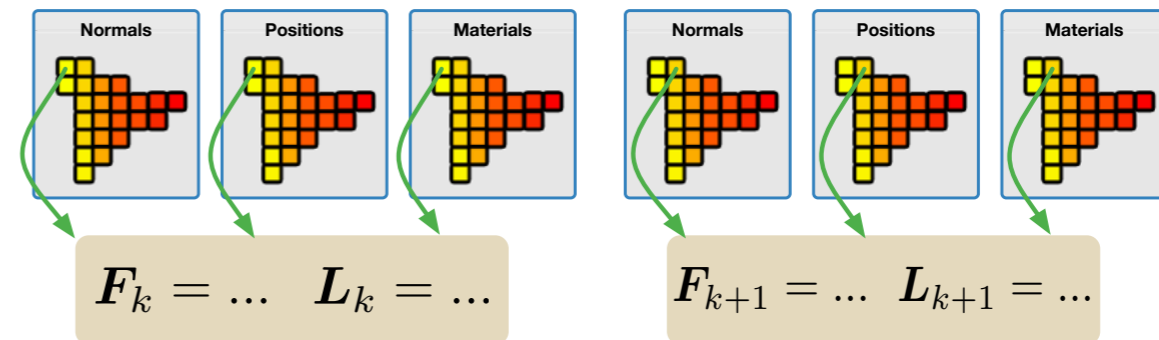
# OpenCL Steps - SRP

- Work Groups (WG) = single GPU core
- Work Item (WI) = thread within WG
- Each WI will perform the SRP computation for a single pixels in the rasterized spacecraft model rendering

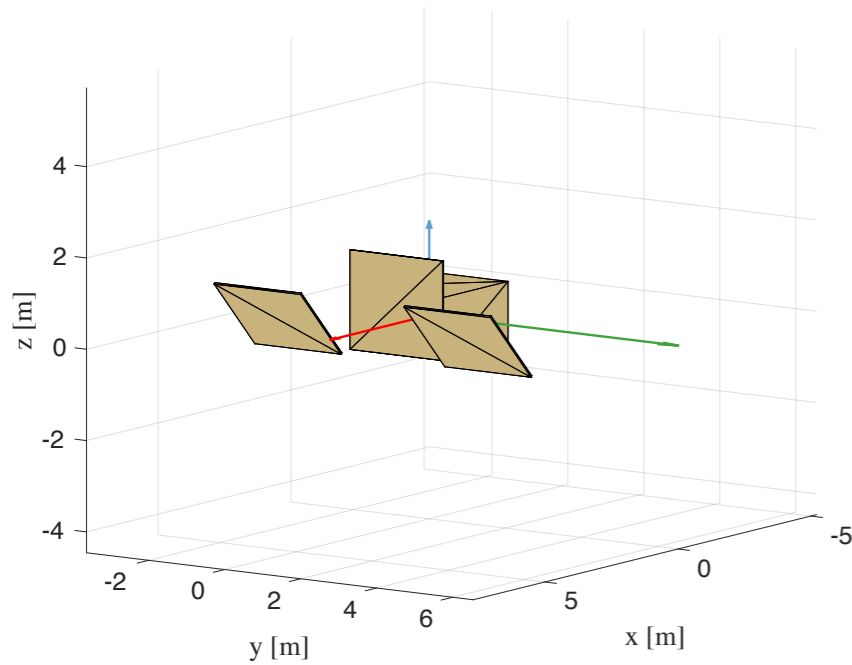


$$\mathbf{F}_{\odot_k} = -P(|\mathbf{r}_{\odot}|)A_k \cos(\theta_k) \left\{ (1 - \rho_{s_k})\hat{\mathbf{s}} + \left[ \frac{2}{3}\rho_{d_k} + 2\rho_{s_k} \cos(\theta_k) \right] \hat{\mathbf{n}}_k \right\}$$

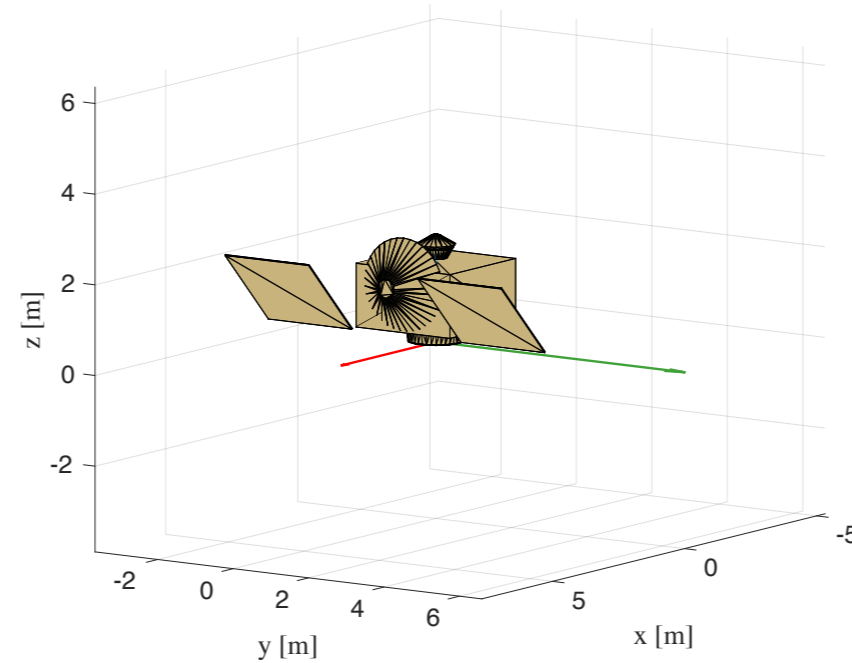
$$\mathbf{L}_{\odot_k} = \mathbf{r}_{P/C} \times \mathbf{F}_{\odot_k}$$



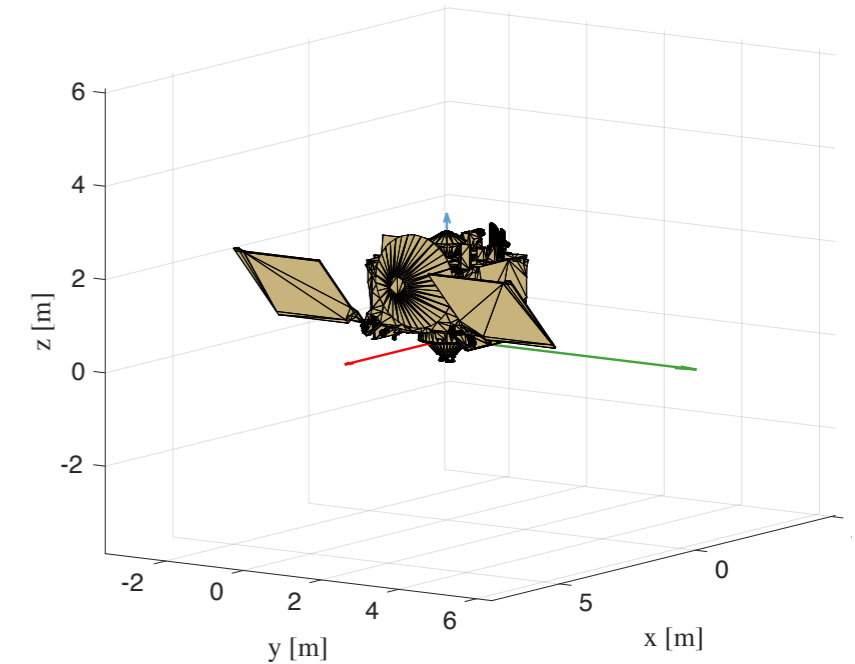
# Mesh Detail Impact



(a) Box and wings.



(b) High gain antenna, thruster ring and sample return module.

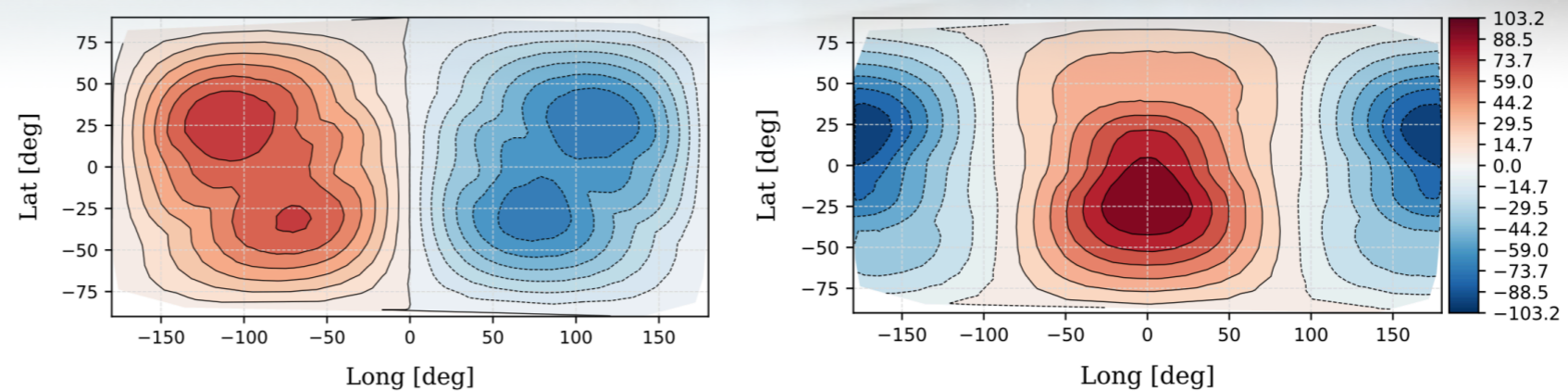
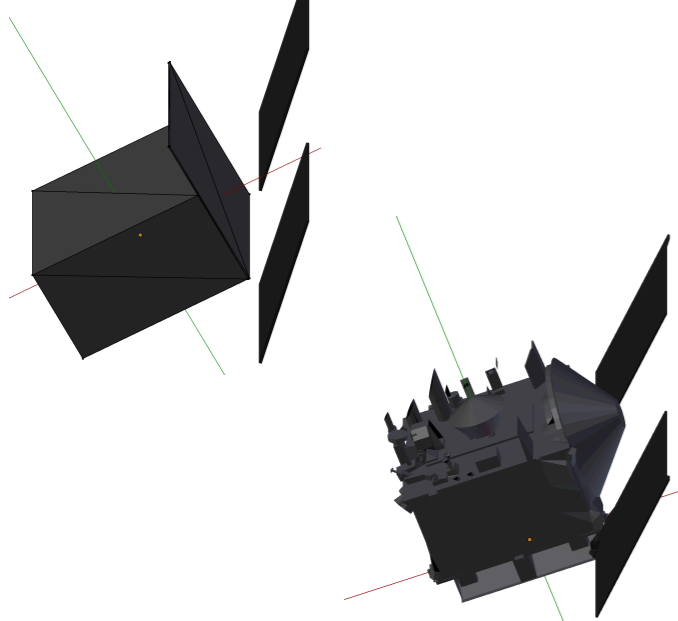


(c) Hifidelity model.

Patrick Kenneally, "Faster than Real-Time GPGPU Radiation Pressure Modeling Methods," Ph.D. Dissertation, Aerospace Engineering Sciences Department, University of Colorado, Boulder, CO, May 2019.

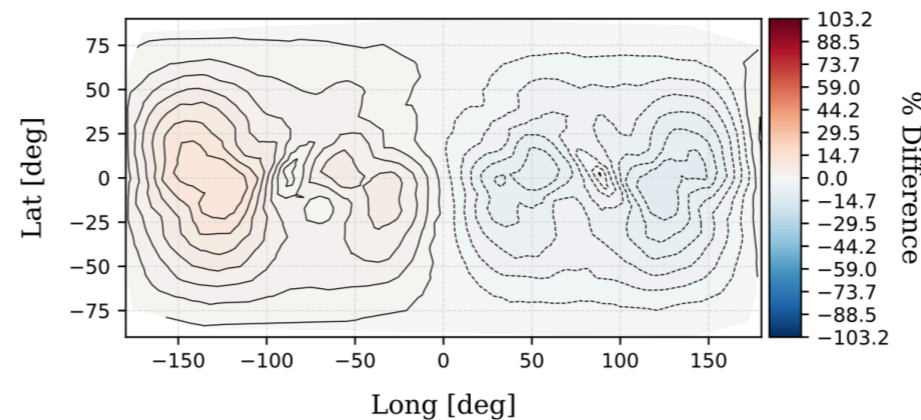
# Torque Box and Wing - Hifi

- Speed means no need to sacrifice resolution with lesser models. So we take a look at what the sacrifice would be if we used other methods to compute box and wing, and flat plate with HGA



(a) Torque  $\hat{x}$  % difference

(b) Torque  $\hat{y}$  % difference

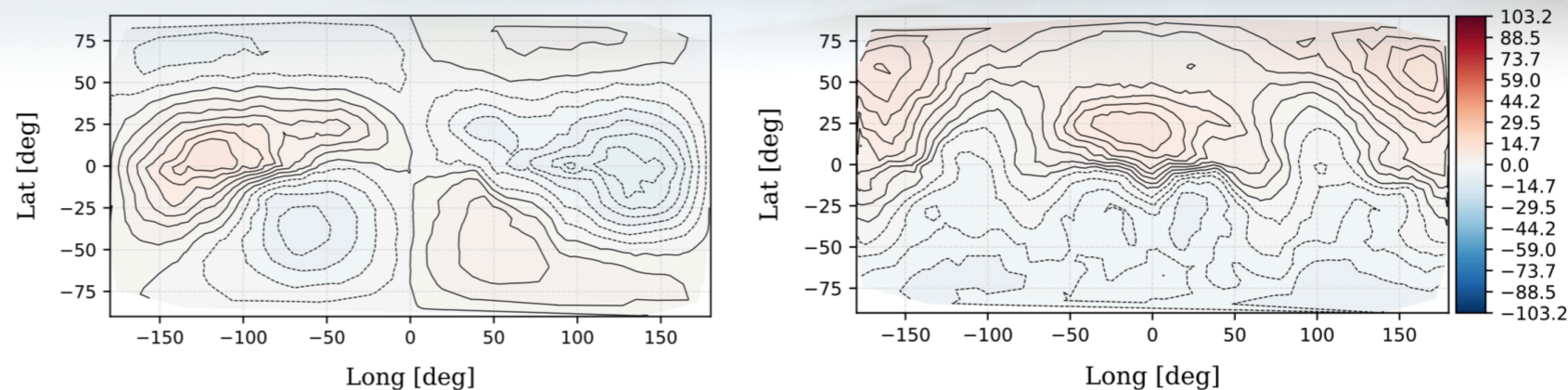


(c) Torque  $\hat{z}$  % difference

Figure 3.17: Torque percentage difference between box and wing model relative to the high-fidelity model with baseline value  $6.57817 \times 10^{-5}$  [Nm].

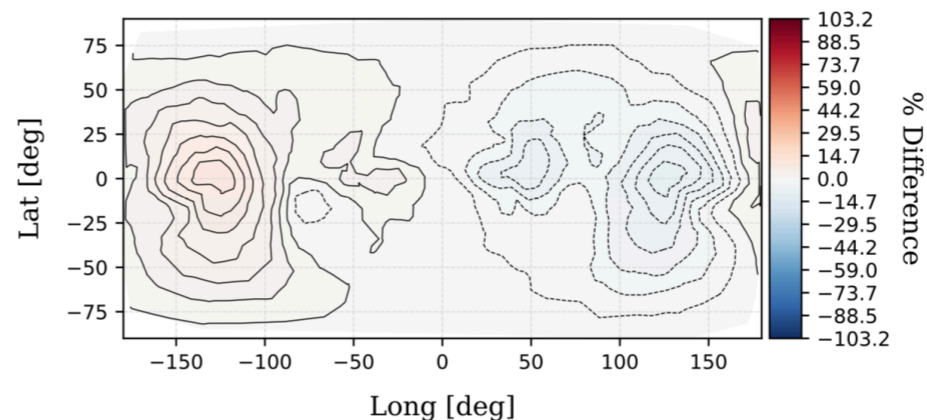
# Torque HGA - Hifi

- Speed means no need to sacrifice resolution with lesser models. So we take a look at what the sacrifice would be if we used other methods to compute torque and wing, and flat plate with HGA



(a) Torque  $\hat{x}$  % difference

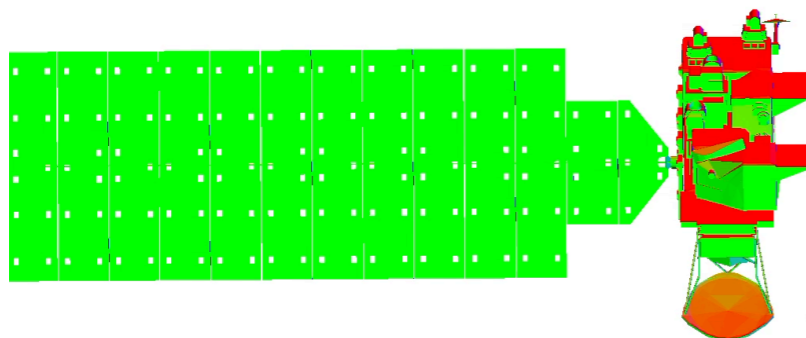
(b) Torque  $\hat{y}$  % difference



(c) Torque  $\hat{z}$  % difference

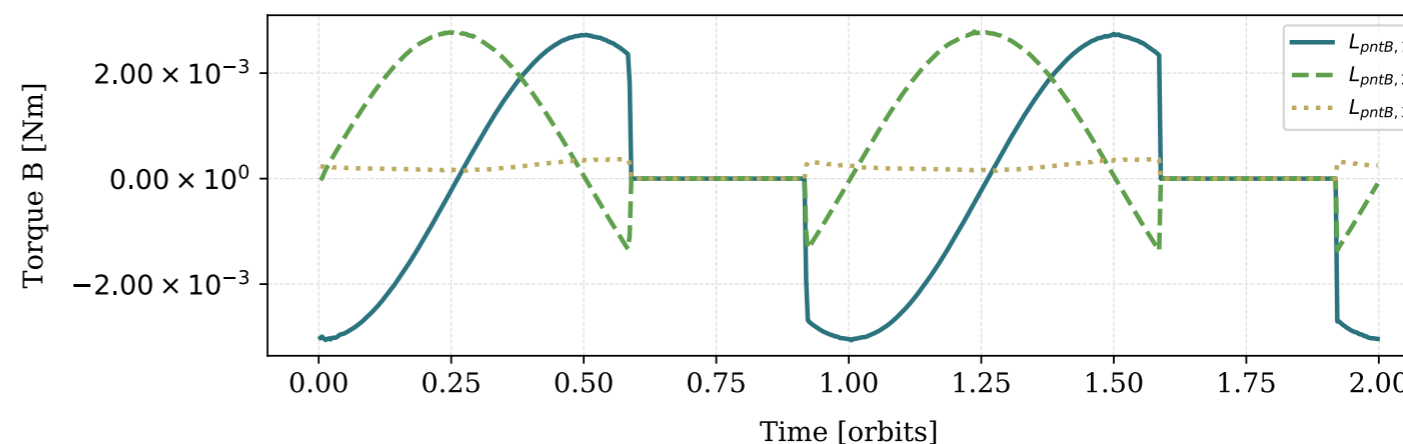
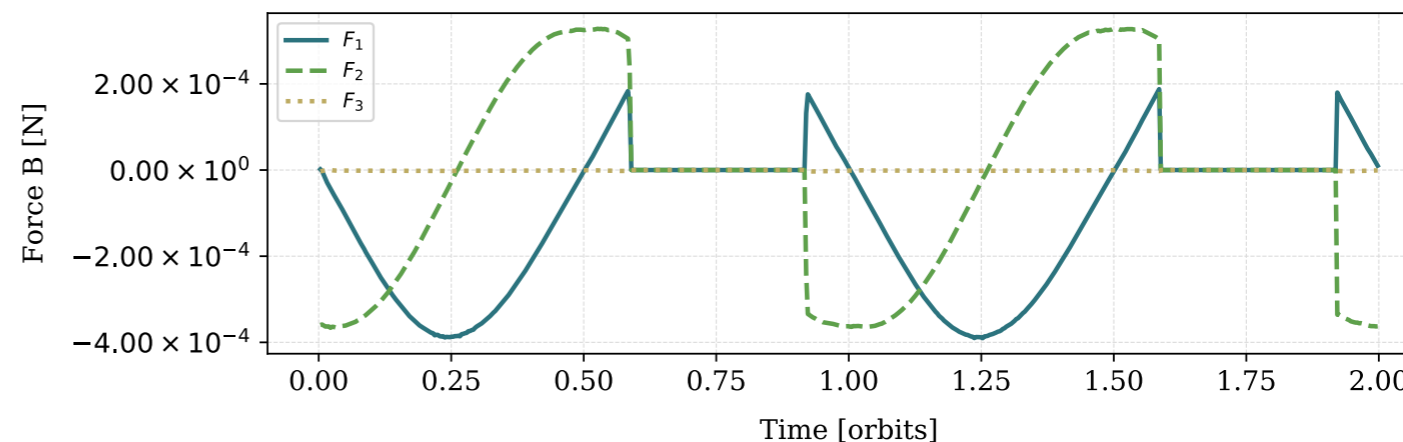
Figure 3.19: Torque percentage difference between HGA model relative to the high-fidelity model with baseline value  $6.57817 \times 10^{-5}$  [Nm].

- Speed means no need to sacrifice resolution with lesser models. So we take a look at what the sacrifice would be if we used other methods to compute box and wing, and flat plate with HGA

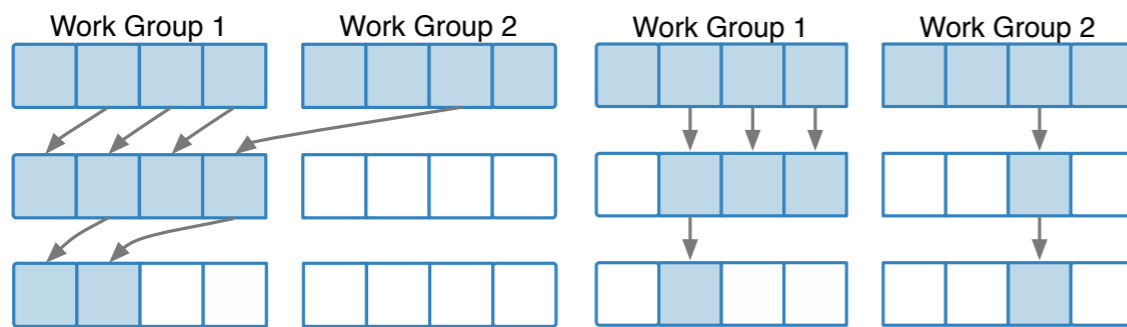
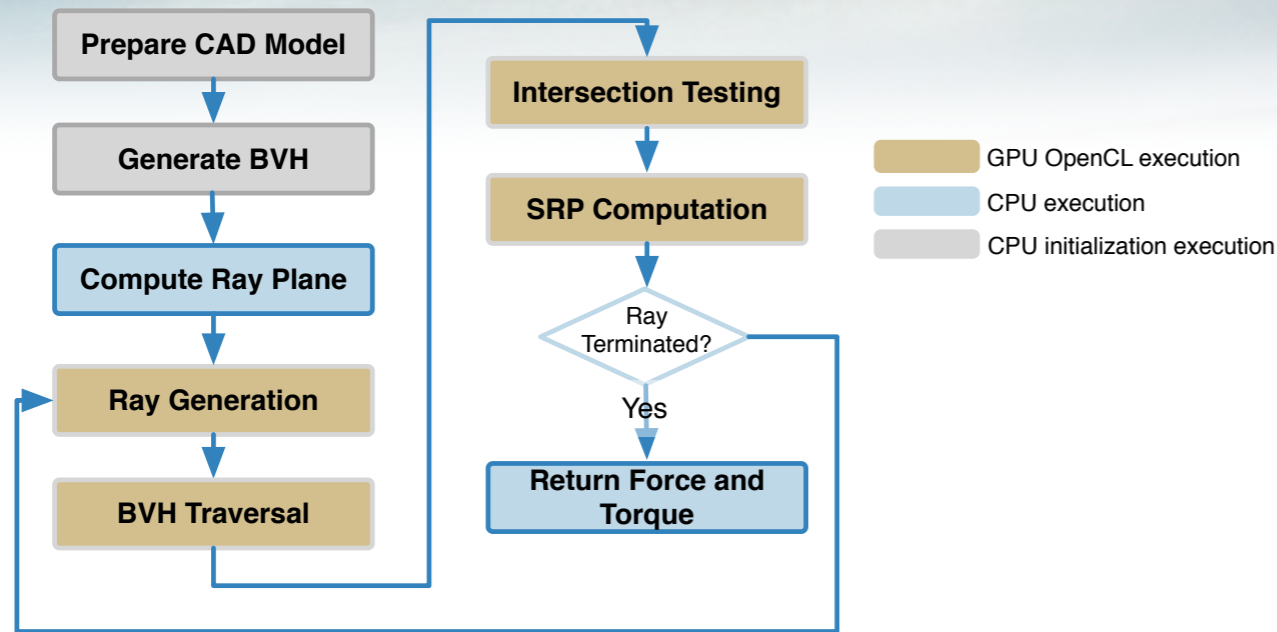


$a$ km	7378
$e$	0
$i$ , deg	90
$M_0$ , deg	90
$\Omega$ , deg	0
$\omega$ , deg	0

Material	Specular ( $\rho_s$ )	Diffuse ( $\rho_d$ )
Gold MLI	0.184	0.736
Silver MLI	0.66	0.16
Germanium MLI	0.3	0.3
Solar array rear	0.1	0.3
Solar array front	0.023	0.092
Solar array boom	0.3	0.3

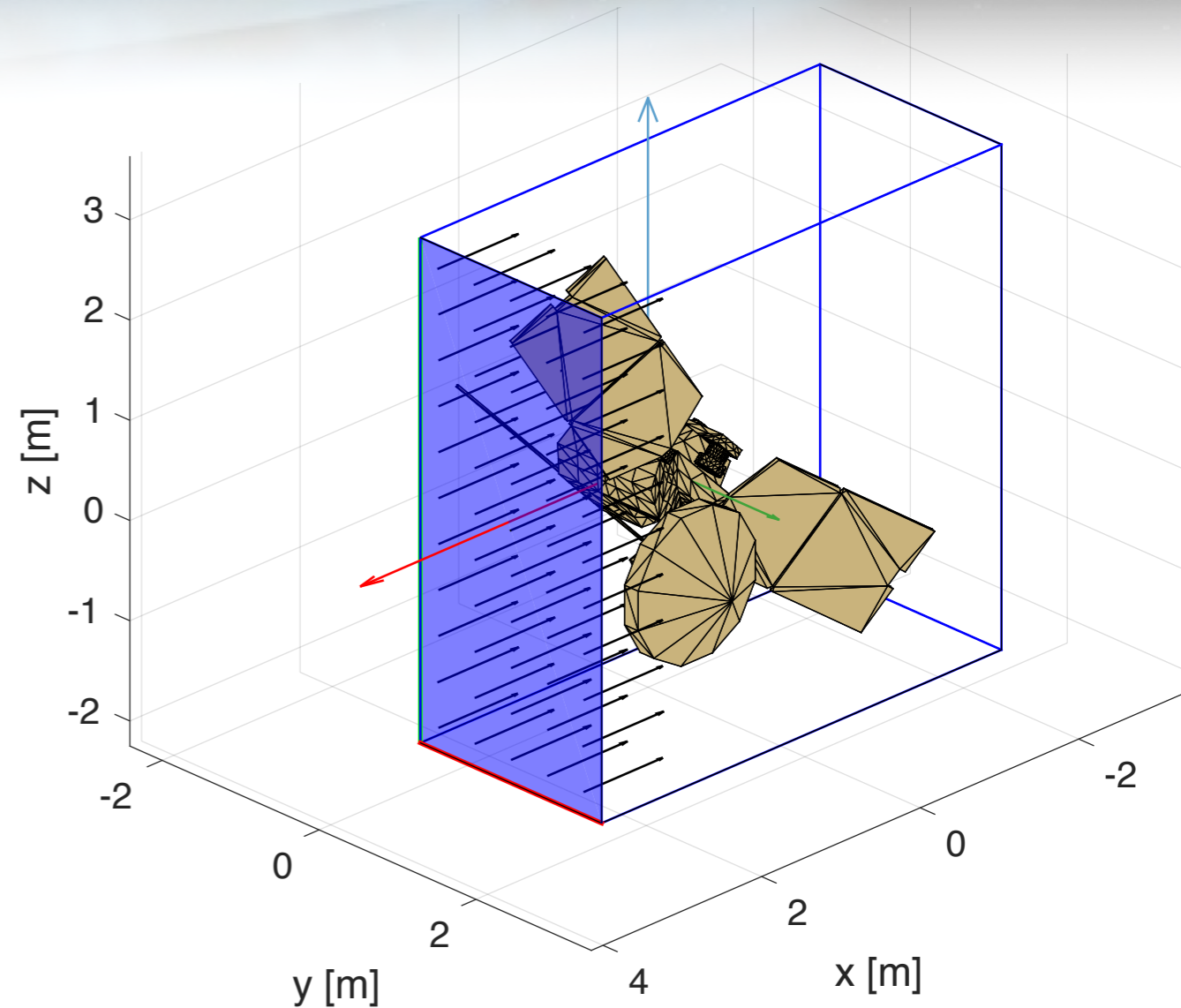


# Ray Tracing SRP Modeling



(a) SIMD by ray

(b) SIMD by pixel

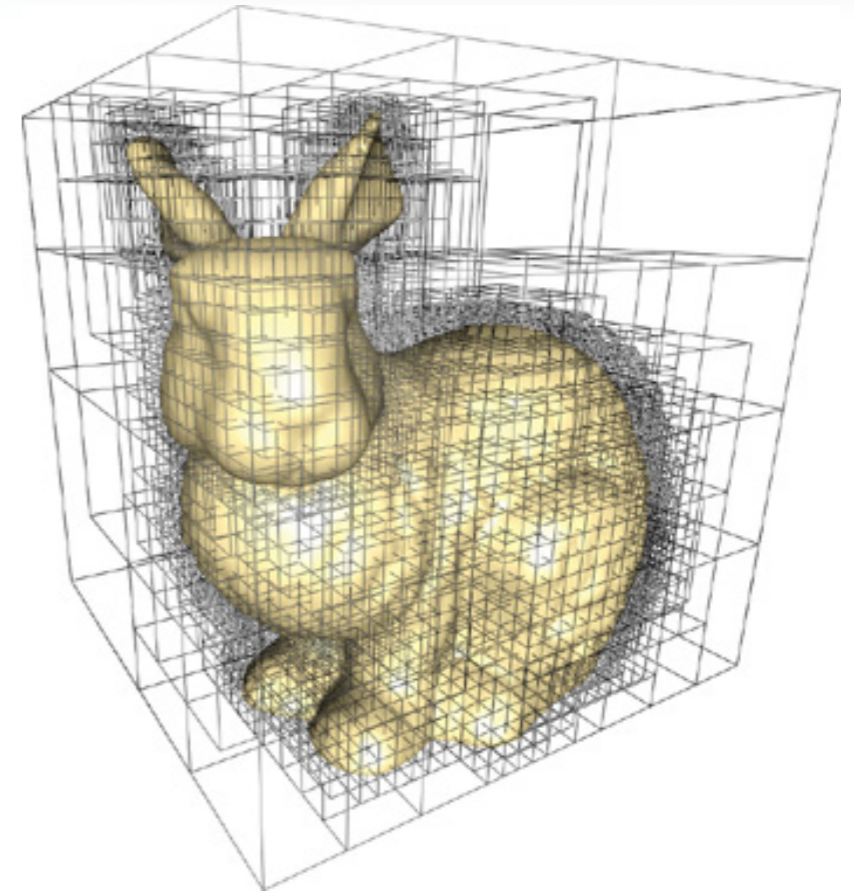
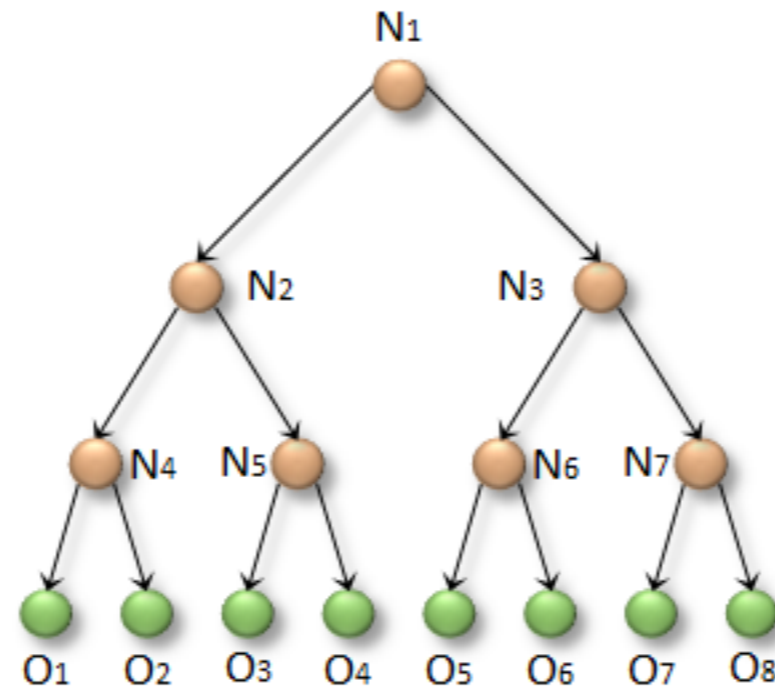
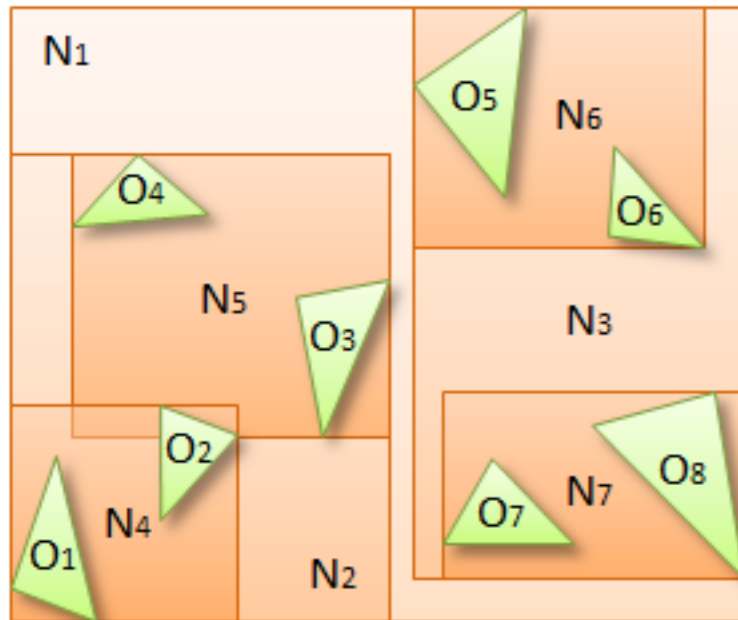


P. Kenneally and H. Schaub, "Fast Spacecraft Solar Radiation Pressure Modeling By Ray-Tracing On Graphic Processing Unit," AAS Guidance and Control Conference, Breckenridge, CO, February 2-7, 2018.



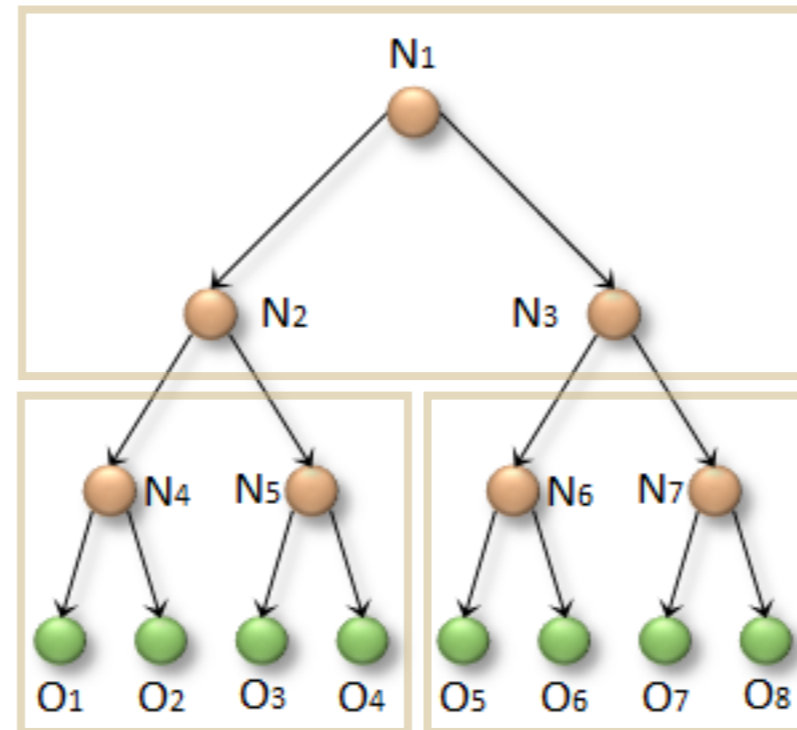
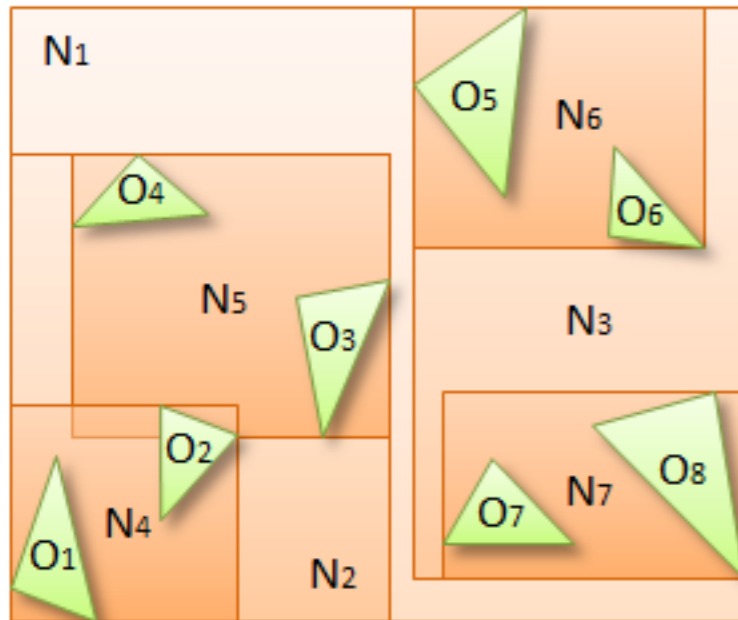
# Bounding Volume Hierarchy

- **BVH Goal:** reduce the ray-object intersection search space



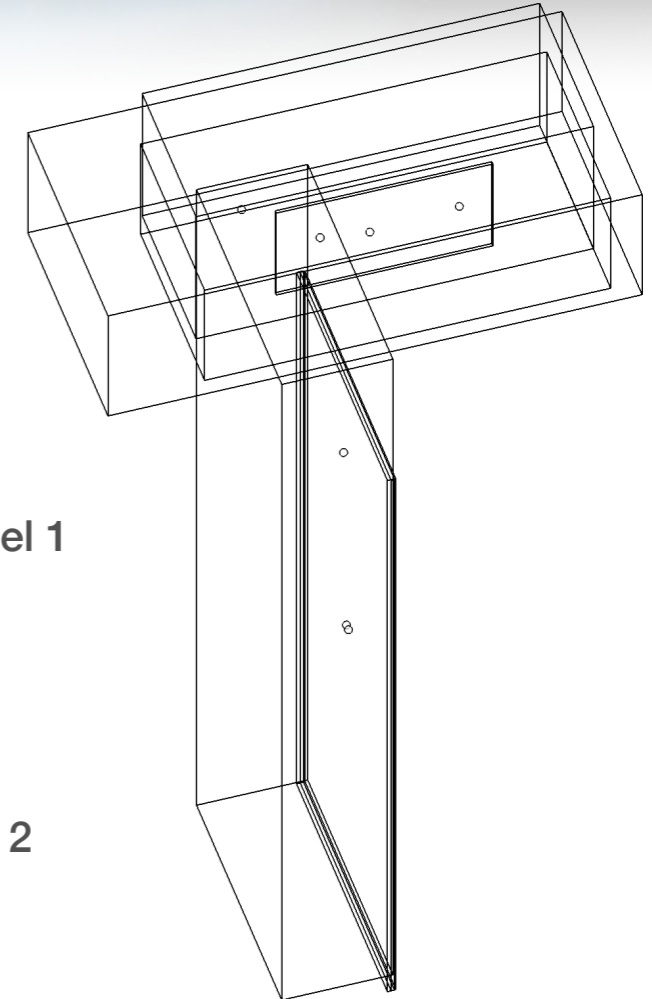
# Bounding Volume Hierarchy

- **BVH Goal:** reduce the ray-object intersection search space
- Two level BVH prevents rebuilding BVH when mesh articulates

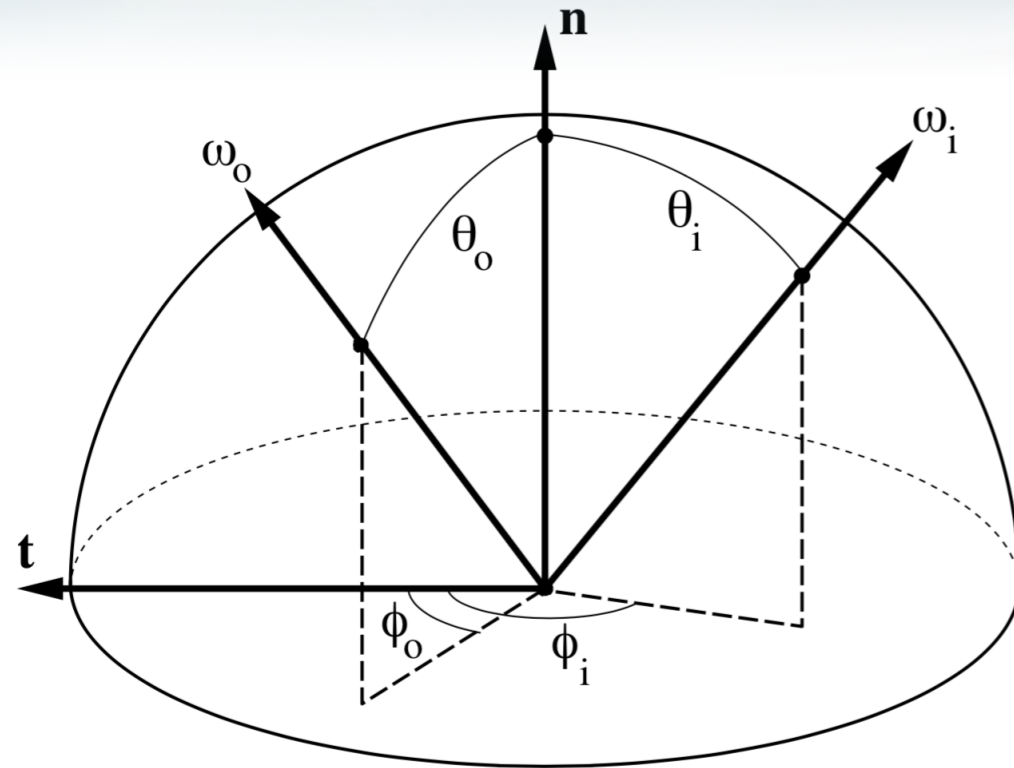


BVH Level 1

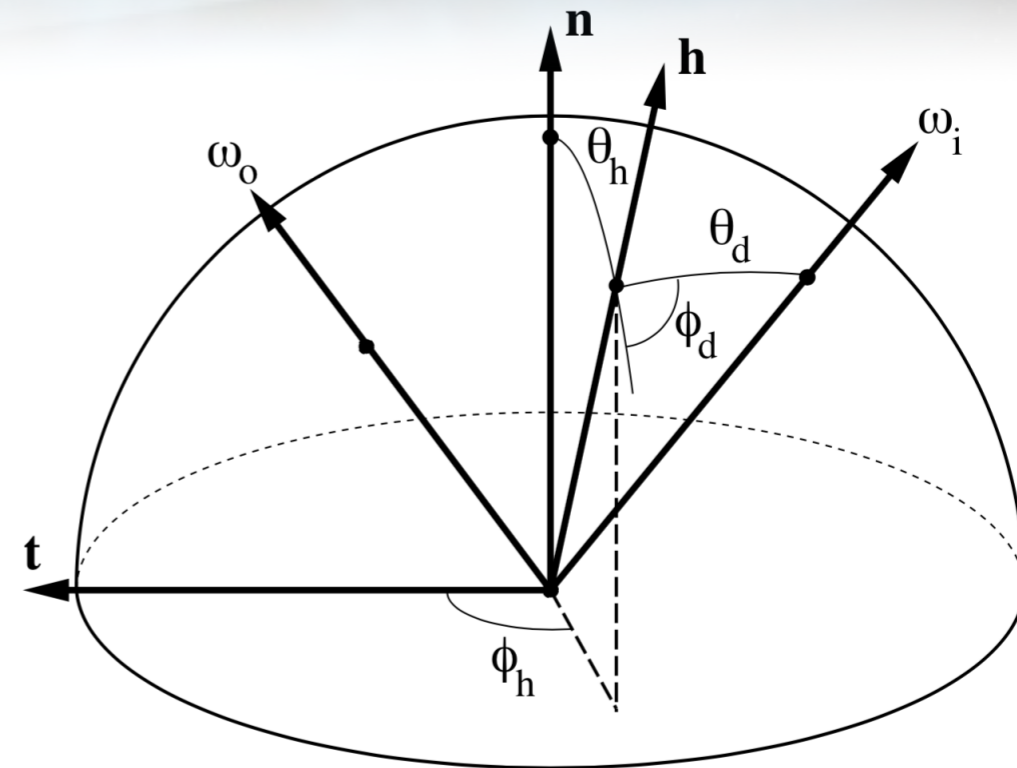
BVH Level 2



# Bidirectional Reflection Distribution Functions



(a) BRDF is parameterized by the intuitive  $(\theta_i, \phi_i)$  and  $(\theta_o, \phi_o)$

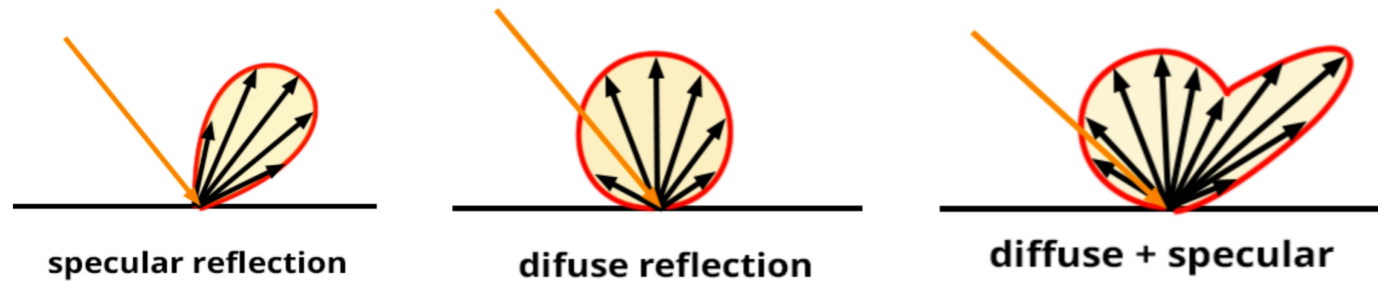


(b) BRDF is parameterized as function of the half angle  $(\theta_h, \phi_h)$  and a difference angle  $(\theta_d, \phi_d)$

P. Kenneally and H. Schaub, "Spacecraft Radiation Pressure Using Complex Bidirectional-Reflectance Distribution Functions On Graphics Processing Unit," AAS Spaceflight Mechanics Meeting, Maui, Hawaii January 13–17, 2019.

# Monte Carlo Evaluation of BRDFs

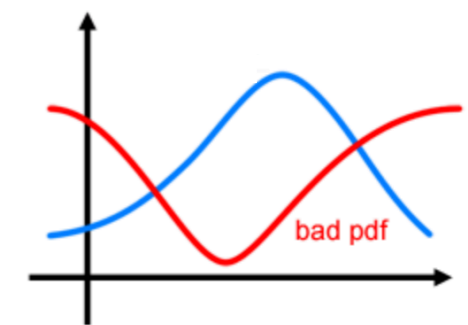
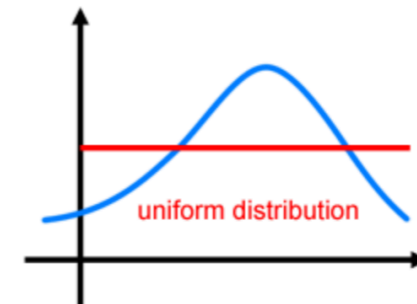
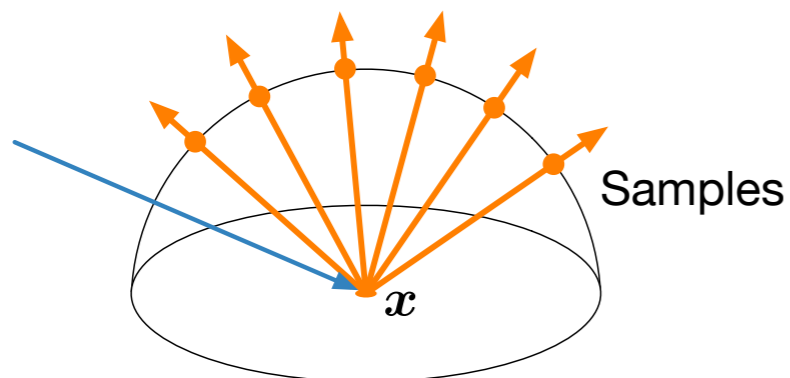
- Evaluation of anisotropic BRDFs can be slow using quadrature



Monte Carlo Estimator

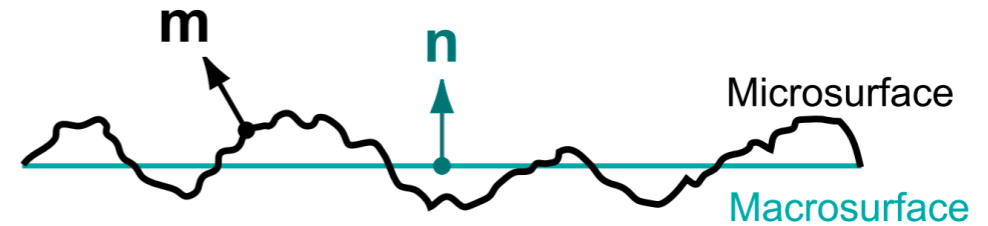
$$\langle F^N \rangle = \frac{1}{N} \sum_{i=0}^{N-1} \frac{f(X_i)}{pdf(X_i)}$$

$$L_o(w_o) = \int_{H^2} L(w_i) f_s(w_i \rightarrow w_o) d\sigma^\perp(w_i)$$



# Microfacet BRDF

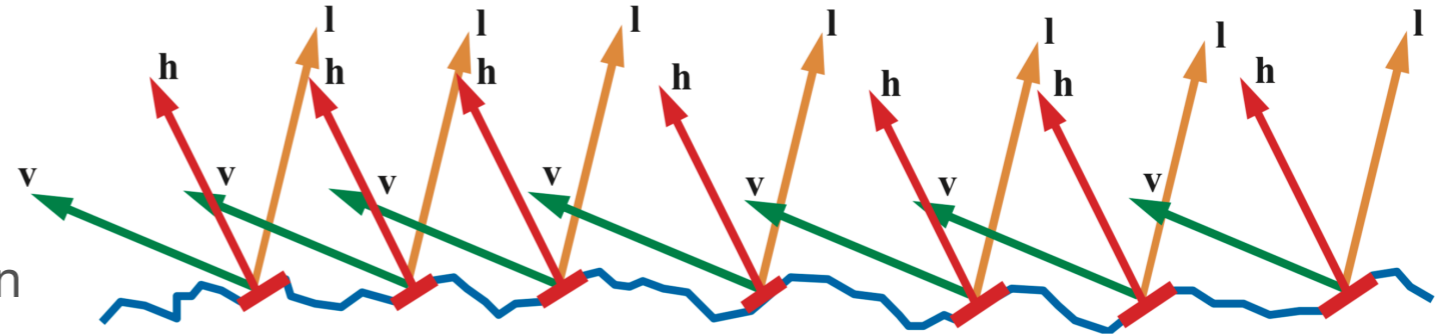
- Surface points with normal  $m = h$  are oriented such that they reflect  $l$  into  $v$
- Other surface points do not contribute to the BRDF.



General micro-facet model

$$R_s = \frac{D(\omega_h)G(\omega_o, \omega_i)F(\omega_o)}{4(\hat{n} \cdot \hat{\omega}_o)(\hat{n} \cdot \hat{\omega}_i)}$$

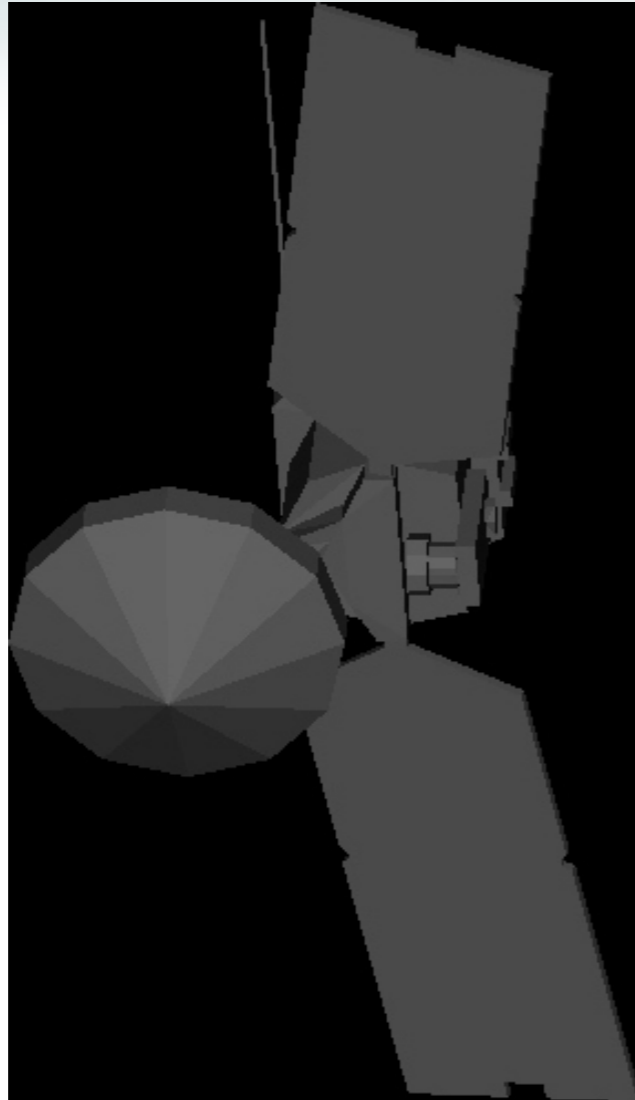
- $D$  is the microgeometry normal distribution function
- $G$  is the geometry function
- $F$  is the Fresnel reflection factor



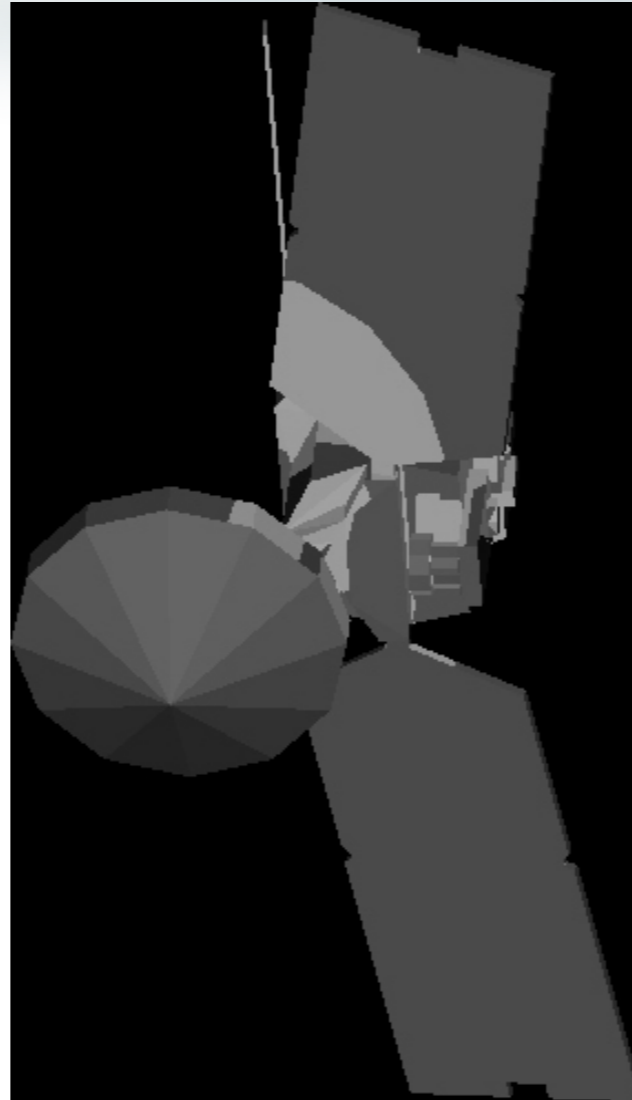
Hoffman, N, « Physically Based Shading Math and Notes »

# Ray Bounce Illustration

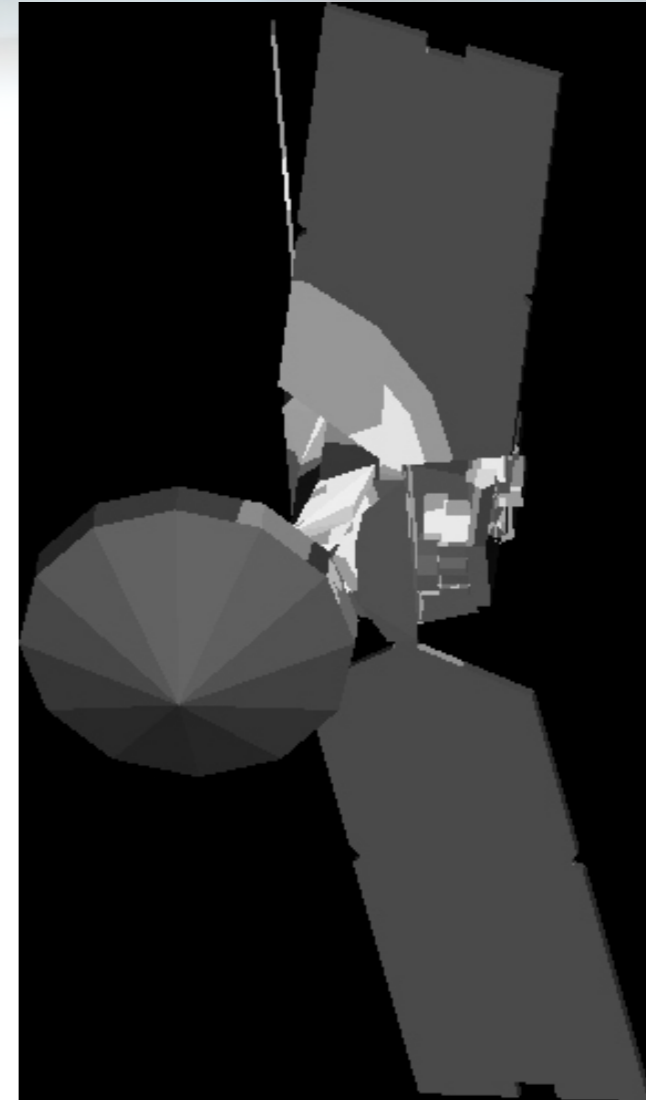
P. Kenneally and H. Schaub,  
"Modeling Of Solar Radiation  
Pressure and Self-Shadowing  
Using Graphics Processing  
Unit," *AAS Guidance,  
Navigation and Control  
Conference*, Breckenridge,  
Feb. 2-8, 2017.



(a) One bounce



(b) Two bounces

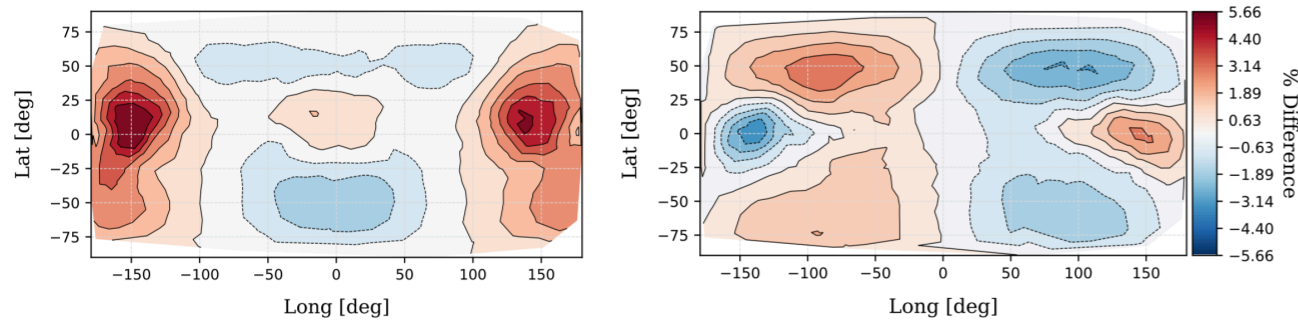


(c) Three bounces

# Multiple Bounce High-Fidelity Model

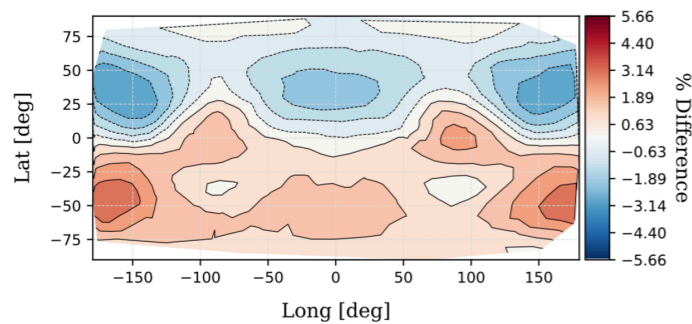
$$F_{i+1, i} = \frac{|F_{i+1}| - |F_i|}{F_{\text{base}}} \times 100 \quad F_{\text{base}} = \frac{1}{N} \sum_{n=1}^N |F_n|$$

$5.62995 \times 10^{-5} \text{ [N]}$

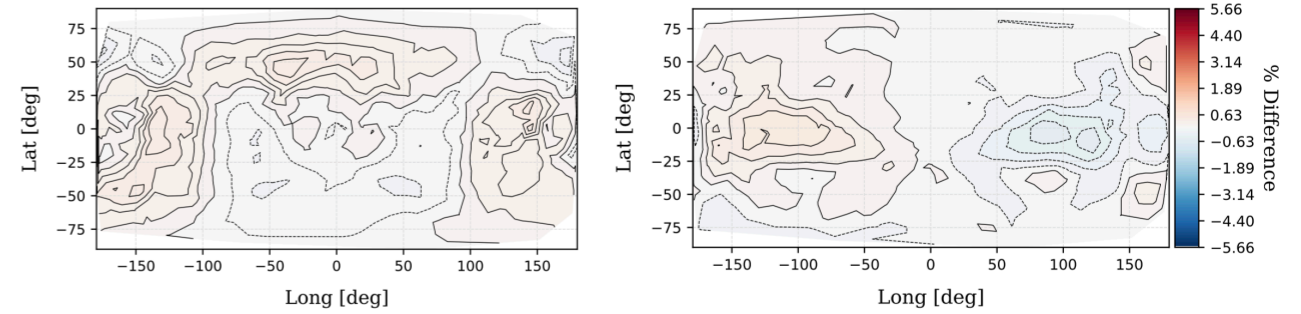


(a) Force x % difference intersection 2 - 1

(b) Force y % difference intersection 2 - 1

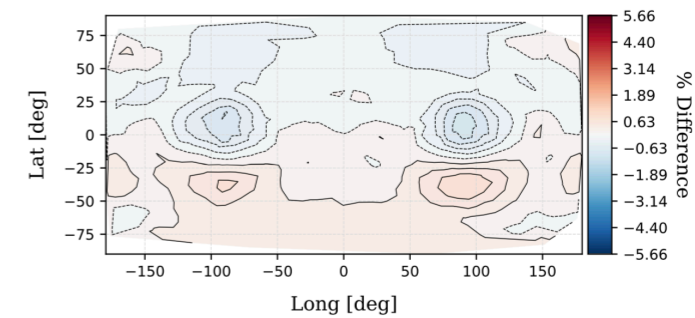


(c) Force z % difference intersection 2 - 1



(a) Force x % difference intersection 3 - 2

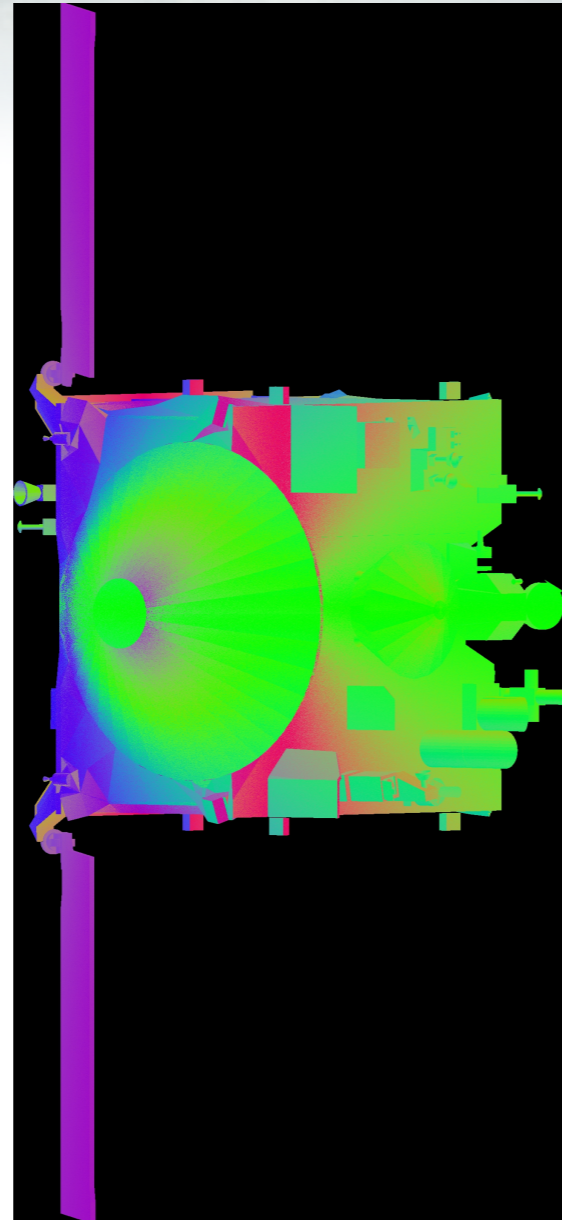
(b) Force y % difference intersection 3 - 2



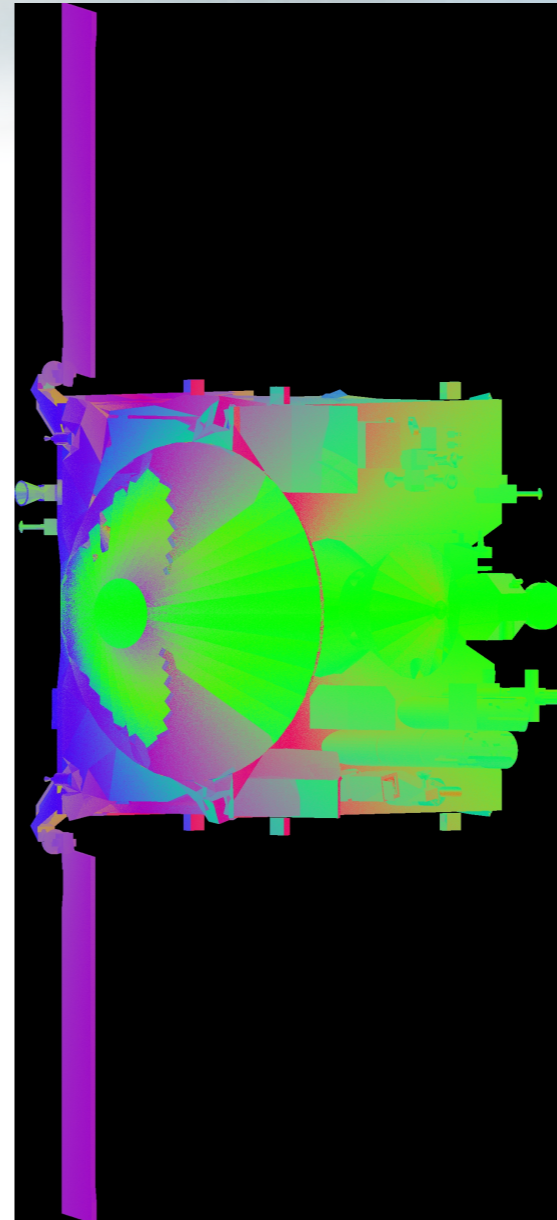
(c) Force z % difference intersection 3 - 2

# Ray Bounce Illustration

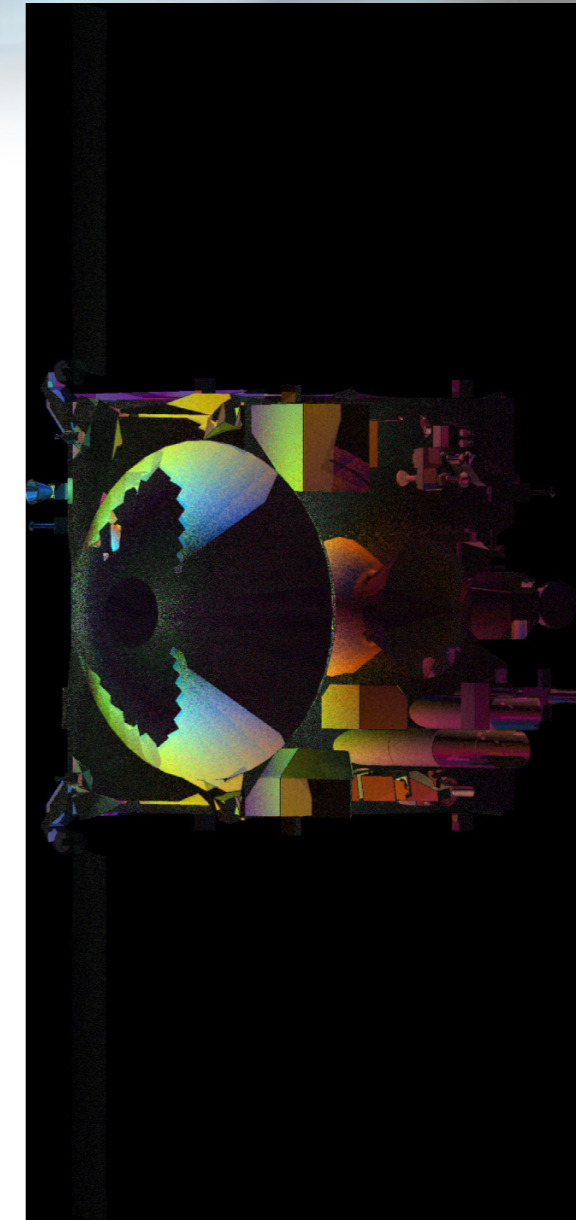
P. Kenneally, "Faster than Real-Time GPGPU Radiation Pressure Modeling Methods,"  
*Doctoral Dissertation, University of Colorado, Boulder, May 2019.*



(a) One bounce.



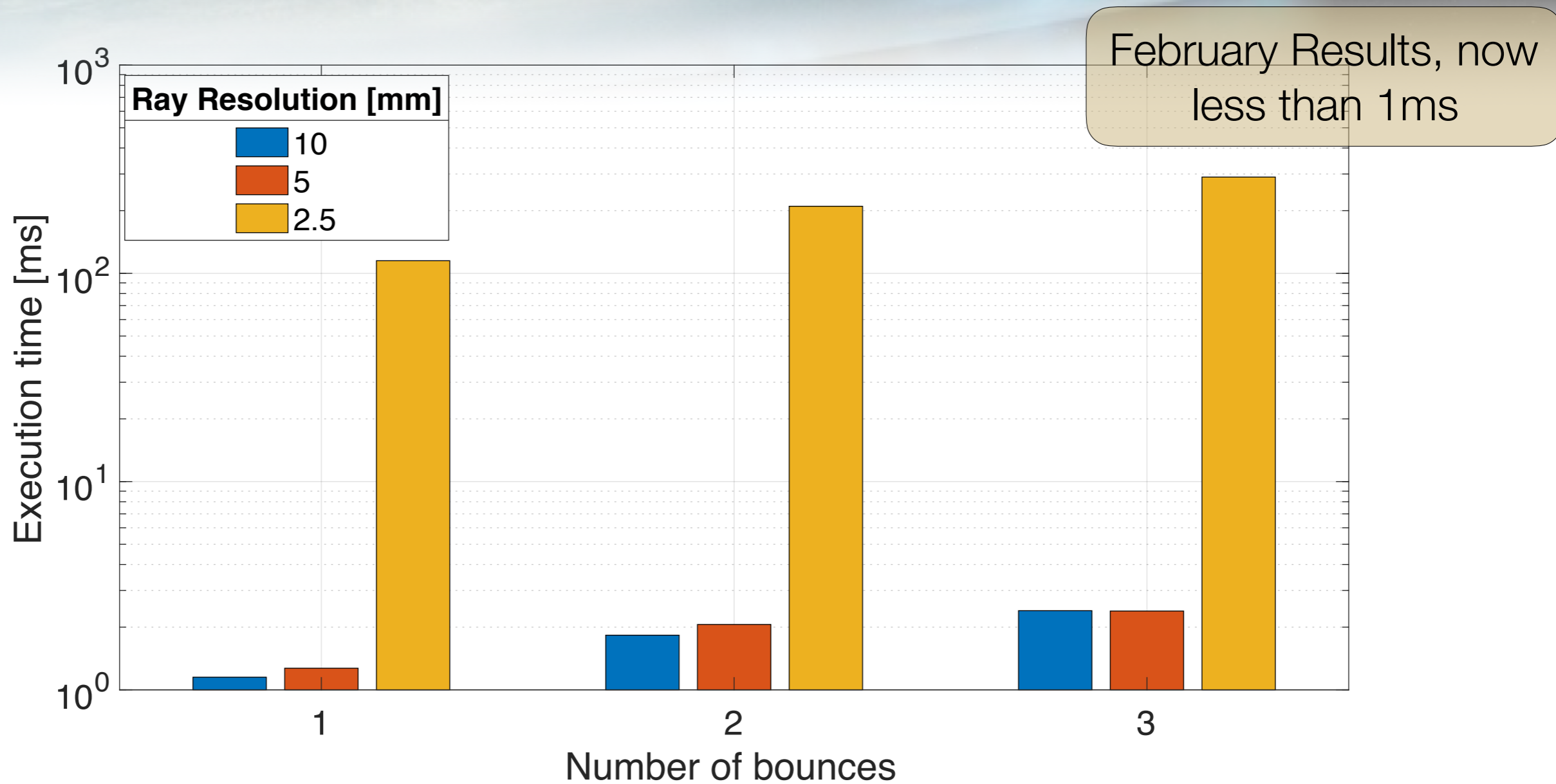
(b) Two bounces.



(c) Image difference.



# SRP Force/Torque Evaluation Comparison



# Execution Times Across Different GPUs

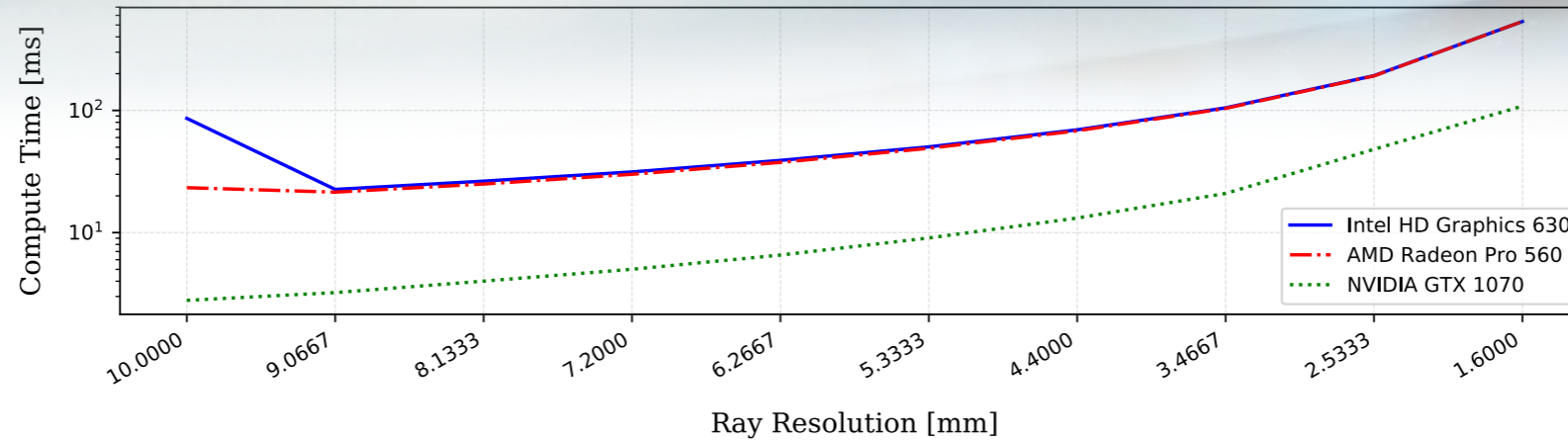


Figure 4.32: Execution times for ray resolutions from 0.01 mm to 0.0016 mm, for one bounce

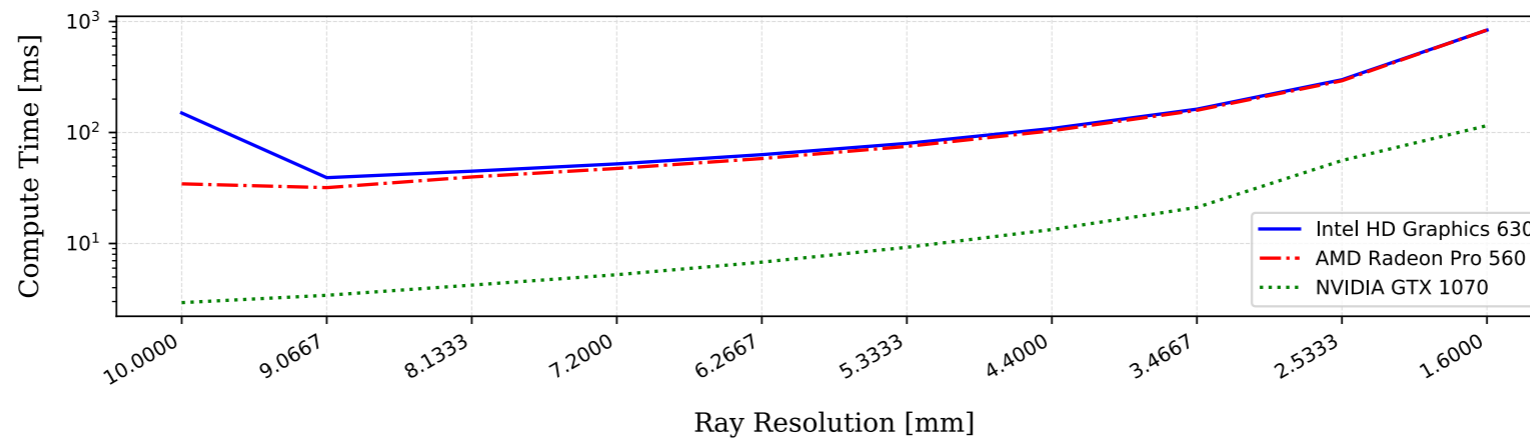


Figure 4.33: Execution times for ray resolutions from 0.01 mm to 0.0016 mm, for a maximum of three bounces.

# Conclusions

- Basilisk's modular natural allows for rapid integration of space environment models
- The current implementation provides convenient base classes for atmospheric neutral density and magnetic field models, as well as the more complex MSIS and WMM models.
- The GPU-based Facet SRP modeling is going to be released shortly in the open *develop* branch. The Ray-Tracing SRP modeling is expected to be incorporated into the open Basilisk repo later in 2020.
- Information about Basilisk can be found at
  - <http://hanspeterschaub.info/basilisk/>



# Questions?